

**Preclinical studies on the novel diagnostic methods  
for canine liver diseases**

(犬の肝疾患に対する新規診断法に関する前臨床的研究)

**Kanemoto Hideyuki**

金本 英之

## CONTENTS

	Page
General Introduction	3
Chapter 1	8
Characterization of canine focal liver lesions with contrast-enhanced ultrasound using novel contrast agent— Sonazoid	
Chapter 2	29
Blood hyaluronic acid as a marker for liver cirrhosis in dogs	
Chapter 3	42
Application of gene expression analysis for clinical diagnosis of canine liver parenchymal diseases	
Conclusion	66
Acknowledgements	70
References	71
Tables	77
Figure legends	90
Figures	97

## **General introduction**

Canine liver diseases include neoplastic and non-neoplastic diseases. Neoplastic diseases of the canine liver can be classified as benign and malignant, and the clinical behaviours of these two are completely different. Most malignant tumors have a worse prognosis, while most benign liver tumors, usually seen particularly in older dogs, are thought to be stable and exert little or no effect on the animals' health status (Balkman, 2009; Liptak, 2007). It is obviously important to distinguish malignant from benign lesions during clinical evaluation. In a similar way, it is also of great value to assess the stage of non-neoplastic liver diseases by clinical or a clinicopathological approach, because dogs with advanced stage non-neoplastic liver disease also have a worse prognosis than those at the earlier stage. In fact, cirrhosis, the end stage of liver disease, has been reported to have a worse prognosis than liver disease without cirrhosis (Poldervaart *et al*, 2009; Sevelius, 1995).

However, as the clinical signs of hepatobiliary diseases in dogs are nonspecific, clinical examinations are important for diagnosis or determination of the stage of the disease. These diagnostic methods range from blood examinations such as liver enzymes, imaging tests, and liver biopsy followed by histological examination. Although the definitive diagnosis should be made by histopathological examination of biopsied tissue, it is impossible to perform liver biopsies in all clinical cases because of its invasiveness and complications including bleeding and problems related to general anesthesia (Rothuizen and Twedt, 2009). Clinicians rely on less invasive diagnostic tests such as blood examinations and imaging, but the information from

these tests is limited. For example, radiography and ultrasound, the two most frequently used imaging modalities in the veterinary field, are not useful to distinguish malignant from benign tumors (Wrigley, 1985). Furthermore, there are no reliable tumor markers available in veterinary medicine, though there are several hepatic tumor markers in humans, such as alpha fetoprotein (Gomaa *et al*, 2009). In non-neoplastic liver disease, the usefulness of imaging modalities depends on the type of disease. Macroscopic vascular disorders (congenital portosystemic shunts) and biliary tract diseases can be detected or diagnosed well using ultrasound or CT (Gaschen, 2009). However, in diffuse liver diseases, these are considered to be less useful (Biller *et al*, 1992; Feeney *et al*, 2008; Gaschen, 2009). Among blood examinations, some biochemistry tests can identify the presence of diffuse liver disease. However, these are non-specific and do not give us information about the stage of the disease (Center, 2007; Hall, 1985; Watson, 2009). In human, a number of serum markers for estimating the stage of liver disease have been proposed and applied to clinical medicine, such as laminin, type I and type III procollagen, and hyaruronan (Gressner *et al*, 2007; Manning and Afdhal, 2008). Novel noninvasive diagnostic tests that are capable of determining the malignancy of tumor lesions or the stage of non-neoplastic diseases are desired.

Even when biopsy can be performed in canine patients with non-neoplastic disease, further problems still exist. One is that the estimation of the stage of the non-neoplastic liver disease, assessed pathologically by the extent of fibrosis, depends on the pathologist, because

the evaluation is subjective (Center, 2007). Standards of histological diagnosis in canine liver disease have recently been established (Cullen, 2009) and this standardization helps to achieve consensus on liver histology in dogs, although it is not enough to improve the subjectivity of histopathological examination. Another problem is that histopathological examination is neither quantitative nor absolute, but rather, both qualitative and relative. In fact, in papers dealing with canine diffuse liver diseases, the severity of the lesion was provisionally described semiquantitatively with various criteria (Mekonnen *et al*, 2007; Poldervaart *et al*, 2009; Shih *et al*, 2007). The third problem is that, because the pattern of fibrosis differs between cases, it is difficult to compare the extent of fibrosis among cases. In other words, canine parenchymal disease should be further classified into detailed disease groups. These problems can explain why the pathological information, except for the presence or absence of cirrhosis, has not been a prognostic factor in canine non-tumor liver disease, especially chronic hepatitis.

Based on these problems concerning clinical examination in canine parenchymal liver disease, I planned in this thesis to develop novel diagnostic tools using imaging, clinicopathological, and molecular biological methods to overcome each problem. In chapter 1, contrast enhanced ultrasound using Sonazoid for diagnosing neoplastic disorders in dogs was considered. In chapter 2, the usefulness of hyaluronate, one of the most hopeful markers for liver fibrosis, as a marker of canine liver fibrosis was examined. In chapter 3, microarray analysis and quantitative polymerase chain reaction were performed to consider the application

of gene expression analysis for clinical diagnosis of canine parenchymal liver disease. Although the methods used in each chapter differ completely, all the work is focused on improving the usefulness of diagnostic methods for canine liver disease.

## **Chapter 1**

**Characterization of canine focal liver lesions with contrast-enhanced  
ultrasound using novel contrast agent—Sonazoid**

## ABSTRACT

In order to evaluate contrast-enhanced ultrasound (CEU) using Sonazoid, a novel contrast medium with a liver-specific phase (Kupffer phase), for differentiation of canine focal liver lesions, two studies were performed.

In study 1, Sonazoid was injected in 5 healthy dogs, and the time course enhancement in the liver parenchyma, portal vein, spleen, and renal cortex was evaluated. In the liver parenchyma and spleen, sustained enhancement was observed from at least 8 to 15 min after injection with the peak at 45 sec (liver) and 20 sec (spleen), whereas in the portal vein and renal cortex, the time course enhancement dramatically decreased after the peak enhancement at 30 sec and 20 sec, respectively. No adverse effect was observed after Sonazoid injection in all the dogs that we examined.

In study 2, Sonazoid was evaluated in clinical cases with focal liver lesions in dogs. Twenty-five dogs with at least one liver mass were given intravenous Sonazoid, and the enhancement pattern in the arterial, portal, and parenchymal phase was characterized. An enhancement defect in the lesion in the parenchymal phase was observed in all malignant lesions, whereas only one of nine benign lesions had a filling defect. The diagnostic value of the presence of a filling defect for malignancy in the parenchymal phase was statistically significant (100% sensitivity, 88.9% specificity, 94.1% positive predictive value, 100% negative predictive

value), and was equal to that of hypoenhancement in the portal or delayed phase. The defect pattern (clear or irregular defect) was significantly dependent ( $P < 0.05$ ) on the types of malignancy (ie., hepatocellular carcinoma and other types of malignancies). In the arterial phase, five of the six hepatocellular carcinomas had hypervascularity, whereas no other lesion was characterized by hypervascularity. In some dogs, additional lesions that could not be observed with conventional B-mode ultrasonography were detected in the parenchymal phase. The enhancement pattern of Sonazoid, especially in the parenchymal phase, has potential as a diagnostic tool for canine focal liver lesions.

## Introduction

Contrast-enhanced ultrasound using microbubble-based agents is useful for detecting and characterizing focal liver lesions in humans (Bolondi *et al*, 2007; Hohmann *et al*, 2003; Konopke *et al*, 2007; Kudo, 2007). There are some reports regarding the contrast-enhanced ultrasound with agents such as SonoVue, Definity, or Levovist (Kutara *et al*, 2006; Nyman *et al*, 2005; O'Brien, 2007; O'Brien *et al*, 2004; Ohlerth and O'Brien R, 2007; Salwei *et al*, 2003, 2005; Szatmari *et al*, 2003; Ziegler *et al*, 2003). SonoVue and Definity are second-generation blood pool contrast agents that remain within the vessels and enable the acquisition of continuous enhanced images with a low mechanical index and contrast harmonic imaging. Levovist specifically enhanced the liver, but the acoustic power requirement was so high that continuous or high-frame rate observation was difficult (Cosgrove and Blomley, 2004; Kim *et al*, 2000).

Sonazoid, a new second-generation contrast agent, consists of an aqueous dispersion of lipid-stabilized perfluorobutane-filled gas microbubbles. The advantage of Sonazoid compared with other agents such as SonoVue or Definity is that it consists of a vascular phase and a true parenchymal phase, or Kupffer phase. The Kupffer phase results from phagocytosis of the agent by the reticuloendothelial system. With Sonazoid, neoplastic tissue is characterized by enhancement defect, probably because of decreased number of Kupffer cells (Watanabe *et al*,

2005; Watanabe *et al*, 2003; Watanabe *et al*, 2007; Yanagisawa *et al*, 2007). Due to this feature, Sonazoid has the potential as an agent for detection and characterization of focal liver lesions, both in humans and animals.

The aim of this chapter is to evaluate the clinical usefulness of contrast enhanced ultrasound using Sonazoid. In study 1, I characterized the image enhancement by Sonazoid in canine liver, spleen and renal cortex and gathered basic information for clinical applications. In study 2, I described the imaging patterns of various canine focal liver lesions using Sonazoid, especially in the Kupffer phase, and clarified the clinical usefulness of Sonazoid in canine neoplastic liver disease.

## Materials and Methods

### Study 1

Five adult beagles, weighing from 11.5 to 13.3 kg with no evidence of hepatic, splenic, or renal disease, were recruited to this study. For each dog, contrast enhanced ultrasound examination was performed with at least five-day intervals. Before contrast sonography, conventional B-mode ultrasound examination was carried out for intended organs and confirmed that there was no ultrasonographic abnormality. Anesthesia was induced by propofol and maintained by isoflurane inhalation after injection of atropine.

Sonazoid (Daiichi Sankyo Corporation, Tokyo, Japan) was intravenously administered at the dose of 0.15ml/head through the cephalic vein as a bolus injection followed by 3 to 5ml 10 % heparin containing saline bolus. The dog was laid in the right recumbent position. The left lateral lobe of the liver and caudal portion of the spleen were demonstrated in each examination. The left kidney was visualized in the spleen survey, if they could be drawn in the same cross section. For ultrasonographic examination, the Aplio XV ultrasound system (Toshiba Medical Systems Corporation, Tokyo, Japan) was used with a convex transducer with a receiving frequency of 3.5 MHz. The mechanical index (MI) was set at 0.2 and all the machine settings were adjusted for contrast enhanced ultrasound using Sonazoid (contrast harmonic imaging mode). The gain setting was adjusted to the minimum extent as the liver parenchyma

was visible. Pictures just before the injection and at 10, 20, 30, 45 sec, every minute from 1 to 15 min, 20 min and 30 min after injection were saved as JPEG files. The region of interest (ROI) was set in each JPEG file for the portal vein, hepatic parenchyma in the liver examination, splenic parenchyma in the spleen examination, and renal cortex in spleen examination, if the kidney was depicted. All the saved pictures were analyzed using the image analysis software Image J (National Institutes of Health, <http://rsb.info.nih.gov/ij/>). The mean gray-scale intensity value (MGD) for each part of all dogs examined was calculated, and the time intensity curve was drawn. All of the statistical analysis in study 1 was done by Wilcoxon test.

Before and after the contrast enhanced ultrasound, physical and blood examination were performed. The complete blood count (total white blood cell count, red blood cell count, platelet count, and hemoglobin concentration), C-reactive protein, blood urea nitrogen, creatinine, alanine aminotransferase, alkaline phosphatase, and albumin were assayed. All the procedures in the study 1 were approved by the ethical committee of the University of Tokyo, and the animals were taken care of humanely.

## Study 2

Cases were recruited if they fulfilled the following criteria: One or more focal liver lesions or a mottled pattern throughout the liver seen using B-mode ultrasound, and a definitive diagnosis made by histologic or cytologic analysis. Twenty-five dogs of various breeds

were included studied. Age ranged from 4 to 11 years old and weight from 2.7 to 31.6 kg. All the patients who underwent surgery had the liver lesion assessed histologically. Hematopoietic tumors such as lymphoma, mast cell tumor, and malignant histiocytosis were diagnosed on the basis of the cytology. In other instances, a histological diagnosis was made by ultrasound-guided 16-gauge needle biopsy or forceps biopsy during laparoscopy, if the lesion was accessible from the surface of the liver. The only exceptions were two dogs with cholangiocellular carcinoma, which were diagnosed by ultrasound-guided needle aspiration. More than two specimens were obtained in all dogs. Diagnoses were made by excision biopsy (n = 8), needle biopsy (n = 8), laparoscopic biopsy (n = 4), and ultrasound-guided needle aspiration (n = 5). The use of the cases in this experiment was permitted by their owners.

Contrast enhanced ultrasound in study 2 was basically performed in the same manner as study 1 except the following modifications to deal with heterogeneous clinical cases. First, 7MHz linear probe was used in the case of lesions that were shallow enough to be depicted clearly, because graphical resolution was better with this probe than the convex probe. Second, contrast enhanced ultrasound was generally performed with patients in conscious state, except for dogs that had undergone computed tomography (CT), which were kept under general anesthesia or sedation. Third, the dogs were laid in the right recumbent or ventrodorsal position, according to the location of the lesion. Fourth, the dosage of Sonazoid was determined as 0.015 ml/kg. Fifth, the protocol by which the observations were conducted was as follows. 0–1

min after the injection, the probe was fixed in a position for imaging. One representative cross-section of the lesion, and the moving picture was recorded. From 1 min to 15 min, whole-liver scanning was conducted in the same manner as conventional ultrasound, and the moving picture or representative picture was recorded.

Three phases (the arterial, portal, and parenchymal) were defined on the basis of the results of study 1: the arterial phase was from 0 to 20 s, the portal phase from 20 s to 1 min, and the parenchymal phase from 8 to 15 min. In the arterial phase, the lesions were classified as hypervascular, isovascular, and hypovascular on the basis of their vascularity, in comparison with the vascularity of surrounding liver. In the portal phase, the perfusion of the lesions was classified as hypoenhanced, isoenhanced, and hyperenhanced in comparison to the surrounding liver. In the parenchymal phase, echogenic enhancements were classified as no defect, an irregular defect, or a clear defect. A defect with central enhancement and a clear border separating it from the surrounding tissue was classified as a clear defect. In contrast, an irregular defect indicated an incomplete enhancement defect with inhomogeneous echogenicity in the lesion. In some cases, only the parenchymal phase was evaluated. By referring to previous reports in human medicine (Brannigan *et al.*, 2004; Catala *et al.*, 2007; Catalano *et al.*, 2005; Dai *et al.*, 2007; Dietrich, 2004; Kim *et al.*, 2000; Migaletto *et al.*, 2004; Nicolau *et al.*, 2006; Suzuki *et al.*, 2003; Tanaka *et al.*, 2001), the vascular patterns of the vessels in the arterial phase were also evaluated and classified as radial, dysmorphic, diffuse homogeneous,

diffuse inhomogeneous, stippled, peripheral, and hypovascular (Figure 1). Among patients with multiple focal liver lesions, the most clearly imaged lesions were selected for evaluation in this study.

The relationship between the enhancement pattern and malignancy or tumor type was analyzed with Fisher's exact test. A *P*value less than 0.05 was considered significant.

## Results

### Study 1

The time course of MGI in the liver was depicted in Figure 2. The hepatic artery was enhanced from 10 sec after injection (data not shown), followed by the beginning of the hepatic preportal vein and hepatic parenchymal enhancement. The portal vein enhancement reached a peak at 30 sec (MGI before and 30 sec after injection is 2.22 and 152.63, respectively), and rapidly decreased thereafter. However, the MGI of the portal vein continued to be significantly ( $P < 0.05$ ) higher than that before injection for 10 min (MGI at 10 sec is 8.45). In contrast, the MGI of hepatic parenchyma reached a peak at 45 sec (MGI = 76.23) and slowly reduced; however, its significant enhancement continued for 15 min (MGIs before and 30 min after the injection are 18.72 and 37.45, respectively,  $P < 0.05$ ). The MGI continued to be higher than that before injection for 30 min (MGI at 30 min is 33.20). The echogenic intensity of the portal vein was significantly ( $P < 0.05$ ) higher than that of the hepatic parenchyma from 20 sec to 1 min, then the intensities reversed, and the MGI of the hepatic parenchyma was significantly higher from 8 min to 15 min after Sonazoid injection.

The time course of MGI in the spleen and kidney was also depicted in Figure 3. The significant ( $P < 0.05$ ) enhancement of the splenic parenchyma compared with that before Sonazoid injection (MGI = 16.45) was observed from 20 sec (MGI = 41.10) after injection and

lasted for 30 min (MGI at 30 min is 31.45).

MGI of the kidney was calculated from 3 of 5 dogs. MGI of the renal cortex dramatically increased with a peak at 20 sec (MGIs before and 20 sec after the injection are 3.79 and 122.74, respectively) and rapidly decreased within 2 min after the injection (MGI at 2 min was 35.03). The significant enhancement continued up to 30 min (MGI was 18.07) as determined by the image analysis ( $P < 0.05$ ).

## Study 2

There were nine benign and 16 malignant lesions. All nine benign lesions were hyperplastic nodules, including hepatic nodular hyperplasias (n = 6) and cirrhotic nodules (n = 3). The 16 malignant lesions included hepatocellular carcinoma (n = 6), cholangiocellular carcinomas (n = 3), lymphomas (n = 2), malignant histiocytosis (n = 1), mast cell tumor (n = 1), leiomyosarcoma (n = 1), liposarcoma (n = 1), and a sarcoma of unknown origin (n = 1). No additional clinical signs or acute allergic reactions including skin or respiratory symptoms were noted during the study.

The findings of conventional B-mode ultrasound are summarized in Table 1. Solitary masses (n = 17) or multiple masses (n=8) were detected in the gray-scale observation. They were hypoechoic (n = 14), isoechoic (n = 2), hyperechoic (n = 1), mixed echogenic (n = 6), or target lesions (n = 2). Eleven dogs were examined with the convex probe and 14, with the linear probe.

The transition of enhancement intensity and vascular pattern in the arterial phase are summarized in Tables 2 and 3, respectively. In the parenchymal phase, the patterns were classified as those representing no defect, an irregular defect, or a clear defect (i.e., an anechoic defect or a defect with a clear border separating it from the surrounding tissue). The target defect, which is characterized by central enhancement with a clear border separating it from the surrounding liver tissue, was included as a clear defect.

In five of the six dogs with hepatocellular carcinomas, hypervascular images were observed in the arterial phase, and in four of these six dogs, hypoperfusion images were detected in the portal phase (Figure 4). A dysmorphic vascular pattern was observed in four of the six dogs with hepatocellular carcinomas. In the parenchymal phase, the presence of an incomplete, irregular, or partial defect was characteristic to all dogs. Weak or incomplete enhancement in comparison with the surrounding tissue was very apparent when moving the probe during the parenchymal phase.

In both of the dogs with cholangiocellular carcinomas that were examined in all three phases, hypoenhancement in the arterial and portal phases was observed. In the arterial phase in two dogs, a stippled, fine vasculature pattern or peripheral, rim-like pattern was observed. In all three dogs with cholangiocellular carcinomas, a clear enhancement defect was apparent in the parenchymal phase. In one dog with cholangiocellular carcinoma, additional focal lesions, which had not been detected with the conventional B-mode ultrasound, were observed in the

parenchymal phase (Figure 5).

The enhancement pattern was almost identical in three different types of hematopoietic tumors including lymphoma, malignant histiocytosis, and mast cell tumor. Hypovascularity and early washout in the arterial and portal phases were characteristic for dogs with hematopoietic tumors. In the arterial phase of the dog with mast cell tumor and another dog with malignant histiocytosis, a peripheral vascular pattern (rim pattern) was observed, and a stippled vascular pattern was observed in a case of lymphoma. In the parenchymal phase, clear defects were apparent in all four dogs with hematopoietic tumors (Figure 6). In one dog with lymphoma, small multifocal lesions became much clearer in the parenchymal phase.

In the patients with leiomyosarcoma and sarcoma of unknown origin, hypovascularity in the arterial phase, early enhancement washout in the portal phase, and a clear enhancement defect in the parenchymal phase were observed (Figure 7). In the dog with liposarcoma, hypoenhancement was observed in the vascular phase and an irregular defect was observed in the parenchymal phase. In one dog with leiomyosarcoma, the presence of additional focal lesions was confirmed in the parenchymal phase. With regard to the vasculature, sarcomas in the arterial phase exhibited a diffuse and homogenous, diffuse and inhomogeneous, or rim pattern.

In contrast to malignant lesions, most benign lesions (in five of the six dogs with

nodular hyperplasia and all three dogs with cirrhotic nodules) had no enhancement defects in the parenchymal phase (Figure 8). In the five dogs with nodular hyperplasia, diffuse and homogenous enhancement patterns with iso or hypoenhancement were observed in the arterial phases; moreover, isoenhancement in the portal phase was consistent in all five dogs. The remaining dog had hypovascularity that was almost anechoic in the vascular phase and clear defects in the parenchymal phase. The enhancement patterns observed for the three dogs with cirrhotic nodules were almost identical in all three phases, although the degree of enhancement was thought to be less than that of the normal liver. The multifocal masses observed by conventional ultrasound became less clear during CEU and almost disappeared in the parenchymal phase. The vascularity was diffuse and homogenous or hypoenhanced.

The pattern of defects in the parenchymal phase was significantly ( $P < 0.01$ ) specific for the pathological diagnosis (ie., irregular defects in hepatocellular carcinoma, clear defects in the other malignancies, and no defects in the benign nodules). Moreover, the hypoenhancement in the portal phase was significantly specific for the malignancy ( $P < 0.05$ ). The sensitivity, specificity, positive predictive value, and negative predictive value of the defect pattern in the parenchymal phase for discriminating histologic or cytologic malignancies from benign nodules was 100%, 88.9%, 94.1%, and 100% for all dogs, respectively. These diagnostic values were 100%, 87.5%, 93.8%, and 100% for dogs which were evaluated in all three phases. These were superior to those of hypoechogenicity in the portal phase for differentiating malignant lesions

from benign ones—86.7%, 50%, 76.5%, and 66.7%—in this study, although there was no statistically significant difference. In the arterial phase, hypervascularity is significantly ( $P < 0.01$ ) specific for hepatocellular carcinoma compared with the other types of lesions.

## Discussion

The true parenchymal phase of Sonazoid is thought to be generated by Kupffer cell phagocytosis (Watanabe *et al.*, 2007; Yanagisawa *et al.*, 2007), which makes it possible to distinguish a malignant from a benign mass because of a lack or a decrease in number of Kupffer cells in neoplastic lesions. In this chapter, enhancement effect of Sonazoid for the liver, spleen and kidney in healthy dogs was examined (study 1) and enhancement pattern of contrast enhanced ultrasound using Sonazoid was also evaluated in 25 dogs with focal liver lesions (study 2). The results indicated that Sonazoid has enhancement effect on hepatic and splenic parenchyma and that the enhancement pattern of the parenchymal phase is as useful as that of the portal phase for differentiating malignant from benign lesions.

In Study 1, basic information of Sonazoid as a contrast agent was gathered before clinical application. First, according to the analysis of temporal enhancement effect, three phases, i.e. the arterial phase (from 0 to 20 sec), portal phase (from 20 sec to 1 min), and the parenchymal phase (from 8 min to 15 min) were defined. The total enhancement duration of Sonazoid in the liver parenchyma lasted for at least 15 min, which was longer than other contrast agents. This difference is thought to be resulted from the efficacies of phagocytosis by Kupffer cells, which is determined by the shell component of contrast agent (Yanagisawa *et al.*, 2007). Second, no adverse effect was observed, suggesting that this agent can be safely

administered to dogs.

In addition, the enhancement effect in the spleen and kidney was also evaluated. The parenchymal enhancement was confirmed in spleen for 30 min and the time intensity curve was almost similar to that of the liver. Although there is no Kupffer cell in the spleen, there is well-developed reticuloendothelial system inside the spleen. The parenchymal enhancement of spleen was thought to be the result of the phagocytosis by this system. Unlike the spleen, the enhancement duration in the kidney is not sustained, probably because of the poor development of the phagocytosis system in the kidney.

In study 2, an enhancement defect in the parenchymal phase was observed in all 16 malignant lesions but only in one of the nine benign lesions, for an 88.9% specificity and a 100% sensitivity. The sensitivity, specificity, and positive and negative predictive values of the diagnostic efficacy of the finding in the parenchymal phase were not statistically different from those in the portal phase, although each value of the parenchymal phase was consistently higher. Thus, with Sonazoid, the finding in the parenchymal phase is as useful as those of the portal phase with regard to discerning malignant from benign lesions.

The arterial phase was also thought to be useful for characterizing tumor type. Hypervascularity was observed in five of the six hepatocellular carcinomas, but not in the other tumor types; this is in agreement with previous reports in animals and humans (Brannigan *et al*, 2004; Kutara *et al*, 2006). The rim sign in the arterial phase, which was reported to be

specific for malignancies other than hepatocellular carcinoma using other contrast agents (Nicolau and Bru, 2004; Xu *et al.*, 2006), was observed in hematopoietic tumors, cholangiocellular carcinoma, or sarcoma. However, this finding was also observed in hepatocellular carcinoma in this study. Tumor size is reported to influence the vascular pattern in contrast-enhanced sonography (Kim *et al.*, 2000). The diagnostic value of the vascular pattern in the arterial phase in canine focal liver lesions should be clarified by conducting a study with a large sample size.

Though the enhancement defect was characteristic for malignant nodules, there was a difference between that for hepatocellular carcinoma vs. other tumor types. In all dogs with hepatocellular carcinoma, the enhancement pattern inside the tumor was characterized by some partial defects, whereas in the other types of tumors there were clear defects. These results are consistent with those of the previous report of Levovist in humans (Tanaka *et al.*, 2001). In this study, the reason for the difference in the enhancement pattern was not known. However, a reduced number of Kupffer cells may still be present in canine hepatocellular carcinoma (Jang *et al.*, 2007), and the Kupffer cells remaining in hepatocellular carcinoma nodules may phagocytose Sonazoid to some extent. More information on resident Kupffer cells in hepatic tumors using immunohistochemical examination and on the functional changes in the Kupffer cells in tumor tissues are required. Two hepatocellular carcinomas did not show hypoenhancement in the portal phase. This is different from that of the previous report using

other vascular-specific contrast agents in which all malignant canine focal liver lesions had hypoenhancement during the portal phase (O'Brien *et al*, 2004). However, in the aforementioned study, only one hepatocellular carcinoma was included. Some hepatocellular carcinomas were reported to sustain enhancement during the portal phase in humans (Jang *et al*, 2007; Tanaka *et al*, 2001). The two hepatocellular carcinomas which showed iso- or hyper-enhancement in the portal phase had hypervascularity in the arterial phase and sustained heterogeneous enhancement in the portal phase. Further studies on a large number of hepatocellular carcinomas is required to clarify the significance of this finding, but combining the findings of all three phases would be helpful in diagnosing hepatocellular carcinoma using Sonazoid.

One of the nine benign nodules, nodular hyperplasia, had hypoperfusion in the portal phase and clear defects in the parenchymal phase. On histologic examination, the nodular hyperplasia specimen was found to be characteristic with normal hepatic tissue structure and cell integrity. The reason for hypoperfusion is unknown.

The overall diagnostic values of Sonazoid for distinguishing malignancy did not reach that of previous report on other contrast agents (O'Brien *et al*, 2004). One of the reasons is that the types of lesions were different. In this study, two hepatocellular carcinomas without portal hypoenhancement and two cirrhotic nodules with portal hypoenhancement were included, which likely reduced the specificity and sensitivity. In contrast, in the previous study, only one

hepatocellular carcinoma was included, and the other types of tumors described here were not included. Moreover, hepatoma, which was included in the previous report, was not included in this study. To compare the diagnostic efficacies of two different agents, studies wherein both types are performed separately are required.

The usefulness of Sonazoid as an ultrasound contrast agent lies in its true parenchymal phase, which continues for at least 7 min. This provides adequate time for examining most of the observable liver without sedation or anesthesia in most dogs. Although the portal phase is as effective as the parenchymal phase for distinguishing malignant from benign lesions, the portal phase or the total vascular phase of other vascular-specific agents lasts only for a maximum of 2 min (Ziegler *et al.*, 2003), which is not adequate for examination of the entire liver in most animals. Levovist, another contrast agent with parenchymal phase imaging of canine focal liver lesions, has been assessed (Kutara *et al.*, 2006). Although the result is the same, in that most of the malignant tumors of the canine liver lack enhancement in the parenchymal phase, Levovist is a hi-MI, first-generation contrast agent that facilitates contrast imaging by destruction of the microbubbles with an ultrasound beam. Moreover, the efficacy of contrast agent uptake by Kupffer cells is lower with Levovist than with Sonazoid (Yanagisawa *et al.*, 2007). Sonazoid is thought to be superior to Levovist because it facilitates continuous and high-frame rate, real-time imaging in the liver-specific phase.

In two dogs with lymphoma, some additional lesions other than the targeted one were

detected during the parenchymal phase that were not observed clearly in the conventional ultrasound. Sonazoid may be useful not only for characterization but also for detection of malignant lesions, though it cannot be confirmed because all the lesions in this study were not examined histologically or cytologically. Further studies comparing the detection accuracy of conventional ultrasonography or other types of agents and Sonazoid would be helpful.

A few limitations exist in this study. First, the number of dogs with each histologic type was small, and there is possibility that the images were not representative of each type of tumor. Second, some important types of tumors, such as hepatoma, hemangiosarcoma, or neuroendocrine tumors were not included. Third, the use of anesthesia has an effect on the time-course enhancement of SonoVue (Nyman *et al.*, 2005); this information is not known for Sonazoid.

## **Chapter 2**

### **Blood hyaluronic acid as a marker for liver cirrhosis in dogs**

## ABSTRACT

Blood hyaluronic acid (HA) concentration was measured in dogs with liver diseases to determine its relationship with histological fibrosis of the liver. The blood HA concentration significantly increased in dogs with chronic liver diseases compared with extrahepatic diseases and healthy control, and the median blood HA concentration in dogs with liver cirrhosis (500  $\mu\text{g} / \text{l}$  range, 151-1970  $\mu\text{g} / \text{l}$ ) was significantly ( $P < 0.05$ ) higher than dogs with non-cirrhotic liver diseases (153  $\mu\text{g} / \text{l}$  range, 15-477  $\mu\text{g} / \text{l}$ ,  $P < 0.05$ ) and was higher in dogs of hepatitis with clinical signs of poor prognosis than dogs without them (380.5  $\mu\text{g} / \text{l}$ , range, 130 – 1970  $\mu\text{g} / \text{l}$  vs. 38.0  $\mu\text{g} / \text{l}$ , range, 15 – 477  $\mu\text{g} / \text{l}$   $P < 0.001$ ). In histochemical analysis, HA was distributed primarily in the fibrotic area in dogs with chronic liver diseases. In conclusion, measurement of the blood HA levels of dogs with suspected liver disease can be a useful diagnostic aid for canine liver cirrhosis.

## Introduction

In the cases of chronic hepatitis or other chronic liver parenchymal diseases in dogs, conventional diagnostic methods such as liver enzymes (e.g., alanine transaminase, alkaline phosphatase), serum total bile acid, and abdominal ultrasound provide some information, but these methods do not always reflect the severity of the disease itself (Watson, 2009).

Histopathological diagnosis is currently the only method that estimates the severity of the disease, which is evaluated mainly by the extent of fibrosis and the degree of inflammation.

However, in the clinical setting, obtaining adequate biopsy samples from patients with liver disease is sometimes difficult due to the risks related to anesthesia and hemorrhage, or due to the owner's preferences. Furthermore, repeated liver biopsies are required to evaluate the progression of the disease and the efficacy of treatment. Similarly, liver cirrhosis, the end-stage of various liver diseases, is sometimes suspected based on symptoms or biochemical profile such as albumin or serum bile acid, but liver cirrhosis is confirmed only by liver biopsy.

Hypoalbuminemia and ascites, frequently observed in dogs with liver cirrhosis, further complicate liver biopsy to perform. Noninvasive diagnostic methods for examining the severity of canine chronic parenchymal liver diseases, especially cirrhosis, are required.

There are a number of blood markers for fibrosis in human medicine. Among them, hyaluronic acid (HA) or hyaluronan in blood is one of the reliable markers for liver fibrosis in

human medicine (Gressner *et al*, 2007; Guechot *et al*, 1996; Pares *et al*, 1996; Plebani *et al*, 1990; Sakugawa *et al*, 2005) and its clinical usefulness has been reported. HA is a component of glycosaminoglycan, a major fraction of the extracellular matrix. The concentration of HA in blood increases as fibrosis develops in patients with liver disease, especially in those with liver cirrhosis (Guechot *et al*, 1996; Pares *et al*, 1996; Plebani *et al*, 1990; Sakugawa *et al*, 2005; Tamaki *et al*, 1996). Although the mechanism underlying this elevation in HA concentration is not fully understood, the synthesis of HA in activated hepatic stellate cells, the main fibrogenic cells in the diseased liver, and the reduced uptake of HA by the hepatic sinusoidal endothelial cells may play important roles (Gressner and Haarmann, 1988; Ichida *et al*, 1996; Tamaki *et al*, 1996; Ueno *et al*, 1993). As the structure of HA is conserved among different species, the assay system used to measure human HA can be used to measure the HA of various species, including dogs (Budsberg *et al*, 2006; Zanna *et al*, 2008). Altered HA concentration in blood has been reported to be related to various pathological conditions, especially osteoarthritis, in veterinary medicine (Arıcan *et al*, 1996; Arıcan *et al*, 1994; Budsberg *et al*, 2006; Nganvongpanit *et al*, 2008; Venable *et al*, 2008; Zanna *et al*, 2008). However, to our knowledge, there has been no report about the relationship between circulating HA levels and hepatic fibrosis in dogs.

In this study, blood HA concentration was measured in dogs with or without various liver diseases including chronic hepatitis, cirrhosis, and primary portal hypoplasia. HA

concentration of dogs with extrahepatic disease was also measured. HA concentration was then compared in each group and to the histological degree of hepatic fibrosis. I also conducted histochemical analysis for HA in these liver specimens to support the idea that a diseased condition of the liver elevates the concentration of HA in blood. Several clinical signs, such as jaundice and ascites, are recently demonstrated as the prognostic factors for shortened survival time after diagnosis of canine primary hepatitis by the multivariate analysis (Poldervaart *et al*, 2009). In this chapter, I also compared HA concentration in dogs with or without these clinical signs to assess the possibility of HA as a prognostic marker in chronic hepatitis which is the most common liver parenchymal disease in dogs.

## Materials and Methods

According to the availability, plasma (n = 7) or serum (n = 18) and liver tissue samples were collected retrospectively from patients who were histologically diagnosed as having chronic liver parenchymal disease. Samples were obtained in Veterinary Medical Center of the Tokyo University, and Animal Medical Center in Nihon University from November 2005 to December 2008. Plasma samples obtained from healthy beagles were used as controls (n = 9). All of the procedures were approved by the ethical committee in the Tokyo University. All the blood sample of dogs with liver disease was obtained before the biopsy procedure or at the first visit after the biopsy procedure in the morning on the empty stomach. Plasma and serum samples were obtained by centrifugation of whole blood, and stored at  $-20^{\circ}\text{C}$  before measurement. Patients were excluded from the study if the size of the biopsy specimens was too small for the evaluation of the degree of hepatic fibrosis. Patients with congenital portosystemic shunt diagnosed on the basis of computed tomography (CT) or abdominal ultrasound examinations were also omitted, because this disease is not a liver parenchymal disease and can be diagnosed clinically by these kind of imaging technique.

The liver tissue samples were obtained from the patients by laparoscopic biopsy or excisional biopsy and were obtained from the control subjects by ultrasonography (US)-guided needle biopsy. At least two separate specimens were obtained in each case. The specimens were

fixed with 10% neutral buffered formalin and were then embedded in paraffin. Sections of the liver tissues obtained from the patients and controls were stained with H & E (HE) and Sirius red to assess the degree of fibrosis. Histological diagnosis was re-evaluated and confirmed from the HE-stained sections, and the severity of fibrosis was evaluated for all the specimens. The liver-diseased dogs were classified into the following two groups: group 1, dogs with hepatic disease without cirrhosis; group 2, dogs with hepatic cirrhosis, i.e. dogs with histological pseudolobule formation characterized by regenerative nodules of hepatocyte and deposition of abundant collagen tissue which is confirmed by Sirius red stain. In liver disease groups (group 1 and 2), histological degree of fibrosis was further classified into five categories (0: absent, 1: mild; with fibrous expansion of the portal area, 2: moderate, 3: severe, and 4: cirrhosis). Healthy beagle dogs and the dogs with extrahepatic diseases were named group 0 and group 3, respectively.

Clinical data including the clinical signs, such as jaundice, ascites and post-prandial serum bile acid concentration, was obtained from medical records.

The HA level was determined using a conventional automated analyzer and a latex-agglutination assay using HA-binding proteins (HABP) (Chichibu *et al.*, 1989; Saito, 2003) in a commercially available kit (Fujirebio, Tokyo, Japan). According to availability, TBA-80FR neo2 (TOSHIBA MEDICAL SYSTEMS CORPORATION, Tokyo, Japan) or BM6050 (JEOL limited, Tokyo, Japan) was used as automated analyzer. Fifty one samples of stored

plasma of patients with extrahepatic diseases which were obtained in the same manner as the liver disease group were randomly collected and HA concentration of these samples was also measured.

HA distribution in the liver was assessed by histochemistry using the biotinylated HABP and avidin-biotin-complex methods. Briefly, deparaffinized sections were treated with 2% hydroxyl peroxide in methanol for 30 min, followed by incubating with 1% bovine serum albumin (BSA, Promega, WI) in 1M phosphate-buffered saline (PBS) at room temperature to block non-specific binding sites. One slide of each tissue was then digested with 10,000 U/ l hyaluronidase from *Streptomyces hyalurolyticus* (Sigma Aldrich Japan, Tokyo, Japan) in 1M PBS for 1 h at 37 °C (negative control). All the slides were incubated with 2 mg/ l biotinylated HABP (Seikagaku, Tokyo, Japan) in 1M PBS for 3 h followed by reacting with 0.25mg/ l peroxidase labeled streptoavidin (Streptoavidin/HRP; Dako, Glostrup, Denmark). HA was visualized using diaminobenzidine solution (500µl/ ml 3-3' diaminobenzidine (Dojindo, Tokyo, Japan) in 0.05 M Tris-HCl buffer (pH 7.6) with 0.3ml/ l hydroxyl peroxide) for approximately 10 min at room temperature.

Steel-Dwass test and Mann-Whitney U test was used for multiple comparison and two sample comparison, respectively. To assess the correlation between extent of histological fibrosis and HA level, spearman's rank correlation test was used.

## Results

This study comprised nine clinically healthy beagles, 25 patients with liver disease, and 51 patients with extrahepatic disease. The control group comprised nine beagle dogs; one male, seven females, and one castrated male; the median and the range of the age was 4 (3 – 6). The patient group comprised 25 dogs (10 males, four castrated males, six females, and five spayed females), aged 1–11 years. The patient group comprised various breeds—American cocker spaniel (7), Doberman (3), Shih Tzu (2), miniature Schnauzer (2), miniature dachshund (1) Beagle (1), French bulldog (2), Labrador retriever (2), Maltese (1), standard poodle (1), Papillon (1), Pembroke Welsh Corgi (1), and mongrel (1). The histologic diagnoses of the patients were liver disease without cirrhosis (chronic hepatitis (9), primary portal vein hypoplasia (6), neutrophilic cholangitis (1), and destructive cholangitis (1), group 1, n = 17) or cirrhosis (group 2, n=8). The median and the range of the age in group 1 and 2 were 6 (4 - 10) and 5.5 (1 – 11), respectively.

The median (range) concentration of HA in the blood was 73  $\mu\text{g/l}$  (19–232 $\mu\text{g/l}$ ) in control beagles; 153  $\mu\text{g/l}$  (15–477  $\mu\text{g/l}$ ), group 1; 500  $\mu\text{g/l}$  (151–1970  $\mu\text{g/l}$ ), group 2; 61  $\mu\text{g/l}$  (18–296  $\mu\text{g/l}$ ), group 3 (Figure 9). The blood HA concentration was significantly different between group 1 vs. 2 ( $P= 0.018$ ), group 1 vs. 3 ( $P= 0.028$ ), group 2 vs. 3 ( $P< 0.001$ ), group 2 vs. the control (group 0) ( $P= 0.03$ , Figure 9). By using the cut-off level of 400  $\mu\text{g/l}$ , the sensitivity,

specificity, positive predictive value, and negative predictive value for liver cirrhosis in patients with chronic liver disease was 75% (6/8), 94.1% (16/17), 85.7% (6/7), and 88.9% (16/18), respectively. The cut-off level was determined by receiver-operator curve analysis using the data of group 1 and 2, because in the clinical setting HA would be measured for patients with suspected liver disease. The point at which the sensitivity and specificity was maximal was adopted as the cut-off level. In comparison, the serum bile acid concentration was not significantly different between dogs of liver disease with and without cirrhosis ( $P= 0.27$ , Figure 10).

The histological degree of fibrosis and blood HA concentration was compared in dogs with liver disease (group 1 and 2, Figure 11). The correlation between HA concentration and the degree of fibrosis was statistically significant but weak ( $P < 0.05$ ,  $R = 0.44$ ).

Dogs with chronic hepatitis and cirrhosis ( $n = 20$ ) were recruited from group 1 and 2 and divided into two subgroups by the presence of clinical signs related to poor prognosis (i.e. ascites and jaundice). The median HA concentration in dogs with these clinical signs ( $n = 12$ ,  $380.5 \mu\text{g/l}$  (130 – 1970  $\mu\text{g/l}$ )) was significantly ( $P < 0.01$ ) higher than that without the symptoms ( $n = 8$ ,  $338.0 \mu\text{g/l}$  (15 – 477  $\mu\text{g/l}$ ), Figure 12)

On histochemical staining of HA in the liver tissue from control dogs, only a weak staining was observed in the portal area. In contrast, much prominent staining of HA was observed inside the fibrotic area in both cirrhotic and non-cirrhotic liver with moderate to

severe fibrosis (Fig. 13). The staining intensities and patterns were not related to the blood HA level (data not shown).

## Discussion

The results of this chapter indicated that the concentration of the circulating HA in dogs with liver cirrhosis is higher than that of dogs with non-cirrhotic liver disease. This result is in part consistent with the reports obtained with respect to humans (Gressner *et al*, 2007; Guechot *et al*, 1996; Pares *et al*, 1996; Plebani *et al*, 1990; Sakugawa *et al*, 2005), and suggests that the concentration of HA in canine blood may be a clinically useful diagnostic tool for dogs and may function as markers of cirrhosis in those with hepatic disease. The significant difference of HA concentration between dogs with negative prognostic factors and dogs without them in chronic hepatitis/ cirrhosis was also shown in this chapter, supporting the idea of clinical usefulness of HA measurement.

HA concentration of dogs with liver disease was significantly higher than the healthy controls and the dogs with extrahepatic disease, but the correlation between blood HA concentration and histological fibrosis was weak. It has been reported that in human, the degree of HA concentration is correlated well to that of histological fibrosis (Gressner *et al*, 2007; Guechot *et al*, 1996; Pares *et al*, 1996; Plebani *et al*, 1990; Sakugawa *et al*, 2005). The reason of that weak correlation was as follows. First, various types of hepatitis were included in this study. Indeed, although there seems to be different types of hepatitis on histological analysis, there is only small number of categories in canine hepatitis for now (Cullen, 2009).

Second, because the number of cases was not enough in this study. These reasons may contribute to the variety of HA concentration and the weak correlation to the degree of the histological fibrosis in dogs with liver disease. Further study with a larger sample size and subdivision of fibrotic stages will be needed to clarify the usefulness of the blood HA measurement for evaluating the degree of liver fibrosis.

HA concentration in chronic hepatitis was compared between dogs with and without clinical signs reported to be worse prognosis. It would be better for evaluation of clinical usefulness of HA to compare the survival time or the response to the therapy between dogs with high concentration of HA and those with low HA level, but larger sample size than that of this study is needed for such kind of analysis.

The results in the histochemical analysis indicated that increased HA in the liver was one of the reasons of elevated circulating HA. However, it was also possible that other factors such as impaired incorporation and degradation of HA from circulation to the liver (Ichida *et al*, 1996; Tamaki *et al*, 1996; Ueno *et al*, 1993) affects blood HA concentration.

In conclusion, this study demonstrated that dogs with liver cirrhosis have elevated blood HA concentrations as compared to those without cirrhosis and that blood HA level is higher in dogs of hepatitis who have worse prognostic factors than those who do not. Measurement of the circulating HA concentration can be an effective and noninvasive diagnostic aid to evaluate the presence or absence of hepatic cirrhosis.

## **Chapter 3**

**Application of gene expression analysis for clinical diagnosis of canine  
liver parenchymal diseases**

## ABSTRACT

Diagnosis of canine parenchymal liver diseases is made based on histopathologic examination; however, quantitative ability and objectivity of the evaluation of pathological specimens are problematic. To establish quantitative and objective tools for examination of canine parenchymal liver disease, I performed gene expression analyses and compared results to histopathologic findings. First, to examine the total gene expression profile in canine liver parenchymal diseases, I performed microarray gene expression analysis using RNA from liver samples of six cases of chronic liver disease and three control samples. Gene expression profiles of all nine samples were divided into three groups by unsupervised clustering: the control group, the chronic hepatitis/liver cirrhosis (CH/LC) group, and the American Cocker Spaniel hepatopathy (ACSH) group. Subsequent pathway analysis showed that gene expression of fibrosis-related genes was increased in both the CH/LC and ACSH groups, although expression of genes related to inflammation were increased only in the CH/LC group. These results were consistent with the histopathologic findings, suggesting that ACSH is a different entity from canine parenchymal liver disease.

Second, to clarify whether quantitative gene expression analysis can be used as a diagnostic tool to estimate the degree of fibrosis, I subjectively selected genes upregulated in the CH/LC group compared to the control group in microarray analysis, namely *COL1A1*, *COL3A1*,

*TIMP1*, *THBS1*, *PDGFD*, *TGFB2*, and *BAMBI*, all of which are biologically related to fibrosis. I performed quantitative reverse transcription polymerase chain reaction (qRT-PCR) using RNA from 15 liver samples of the canine CH/LC and four control samples. Expression levels of all the genes quantified were correlated well with the histological degree of fibrosis, and multiple regression analysis showed quantities of *PDGFD* and *THBS1* expression could predict histologic degree of fibrosis ( $R^2 = 0.75$ ,  $P < 0.001$ ). Furthermore, expressions of these genes were higher in cases with negative prognostic factors than those without these factors. These results show that RNA quantities of liver biopsy measured by quantitative PCR (qPCR) can be used as a quantitative and objective diagnostic tool for estimation of the stage of chronic hepatitis.

## Introduction

Recently, gene expression analyses have been used for the diagnosis, classification, and prediction of disease outcome in humans (Sandvik *et al*, 2006). Gene expression can provide support to the traditional diagnostic methods of laboratory medicine, because it reflects both temporary and lasting changes in tissues. Among the analyses available, quantitative reverse transcription polymerase chain reaction (qRT-PCR) and large-scale gene expression profiling, such as DNA microarray analysis, are important. With these methods, genes related to the pathogenesis of a disease or that reflect a specific pathophysiologic condition can be easily selected and quantified.

Most previous studies regarding the clinical application of gene expression analysis have focused on cancer, with only a few reports on other diseases (Sandvik *et al*, 2006). There are no reports examining gene expression analysis as a diagnostic tool for canine parenchymal liver disease. However, this disease is well suited for this technology because lesions are usually uniform around the liver. Chronic hepatitis (CH) is a common parenchymal liver disease in dogs. The gold standard for the diagnosis of CH is histopathology (Poldervaart *et al*, 2009; Zawie and Gilbertson, 1985), and the stage of the disease is determined by the degree of histologic fibrosis. Although fibrosis is believed to be prognostic in canine CH, no evidence has identified histological fibrosis as a prognostic factor, although some research has shown that

cases with cirrhosis had a worse outcome than non-cirrhotic cases (Poldervaart *et al.*, 2009). In addition, histological estimation lacks objectivity and does not provide quantitative information.

Another problem associated with histopathological examination is that the classification of canine chronic liver disease has not been fully standardized, which leads to different disease variations being classified into the same category. Among these categories, the American Cocker Spaniel hepatopathy (ACSH) represents a recently proposed disease entity among canine chronic liver diseases (Sakai, 2007). ACSH is clinically characterized by portal hypertension, hypoalbuminemia, and coagulation disorders, suggesting that many cases are in hepatic failure at the time of diagnosis. However, the prognosis seems to be better than in other cases of canine CH, in which most cases of hepatic failure are associated with a short survival time (Poldervaart *et al.*, 2009). Histopathologically, ACSH is reported to show spindle-shaped cell infiltration and fibrosis between severe degenerated hepatocytes throughout the liver without severe inflammation. No disease that resembles ACSH has been reported in other breeds. According to its clinical course, histopathologic findings, and breed specificity, ACSH can be considered a unique entity of liver disease in dogs [ ]. To demonstrate its unique pathogenesis, ACSH should be characterized based on factors other than clinical or histologic findings.

To show the usefulness of gene expression analyses as a diagnostic and differential tool for canine parenchymal liver diseases and future clinical application to improve current diagnostic approaches, I conducted two studies. First, I performed microarray gene expression

analysis for canine CH and CH-like lesions, namely ACSH, to show differences in gene expression levels in these diseases and to identify up-regulated genes related to fibrosis in canine liver disease. Subsequently, I conducted qPCR analysis of these candidate genes using a larger number of CH samples and compared expression levels to the histologic degree of fibrosis.

## Materials and Methods

### Sample collection

Dogs previously diagnosed clinically and histologically as having canine chronic hepatitis/liver cirrhosis (CH/LC) that had been referred to the Veterinary Medical Center in the University of Tokyo or Nihon University Animal Medical Center and beagle dogs, as controls (CONT), were included in the present study. American Cocker Spaniels clinically and histologically consistent with ACSH were also recruited. Liver tissue samples were taken using a laparoscopic forceps biopsy technique. Two or more samples were immediately dipped into 10% neutral buffered formalin, and 1 sample was placed into 1 ml RNA later solution (Ambion, Austin, TX, USA) or liquid nitrogen. Formalin-dipped samples were fixed and embedded in paraffin for histologic examination. RNA later-dipped samples were stored at 4 °C overnight and stored at -80 °C until RNA extraction. Fresh frozen samples were immediately stored at -80 °C, treated with RNA later ICE (Ambion) and stored until use. The use of the beagle dogs in the present study was approved by the ethics committee of the University of Tokyo, and the use of the samples obtained from the cases was permitted by the owners.

### RNA extraction

For RNA isolation, samples were thawed on ice, cut to 25–30 µg, and homogenized in 600 µl RLT buffer (Qiagen, Germantown, MD, USA) with Tissue Rupter (Qiagen). RNA was extracted using the RNeasy mini kit (Qiagen) according to the manufacturer's protocol. Extracted RNA was then treated with DNase I (Invitrogen, Carlsbad, CA, USA) and reverse-transcribed using the PrimeScript RT reagent kit (Takara Bioscience, Tokyo, Japan) according to the manufacturer's protocol. RNA grade was confirmed as appropriate for subsequent analysis by gelelectrophoresis.

#### DNA microarray and array data processing

Three control RNA samples, three samples of CH/LC with severe fibrosis, and three samples of ACSH were used for microarray analysis.

RNA samples were converted to biotinylated cRNA and hybridized to Affymetrix (Santa Clara, CA, USA) oligonucleotide microarray (Canine 2.0 genome array) using standard affymetrix protocols.

The raw fluorescence data, that is, CEL files, were preprocessed and normalized to the Robust Multiarray Analysis (RMA) method using the R Bioconductor package, “affy” and “rma” (<http://www.r-project.org/>).

#### Quantitative PCR and statistical analysis

Candidate genes for markers of fibrosis were selected based on the results of a microarray study and included *COL1A1*, *COL3A1*, *TIMP1*, *THBS1*, *PDGFD*, *TGFB2*, and *BAMBI*, which were upregulated in the CH/LC group compared to the CONT group and biologically relevant to fibrosis. *RPL13A* and *RPL32* were used as internal control genes.

Genes were quantified in duplicate with Thermal Cycler Dice Real-time System (Takara Bio Inc., Tokyo, Japan) with SYBR premix EX taq (Takara Bio Inc.) or SYBR II premix EX taq (Takara Bio Inc.) on 96 well plates and film according to the manufacturer's manual. The primers were designed using Primer 3 (<http://primer3.sourceforge.net/>), PrimerExpress (Applied Biosystems, Carlsbad, CA, USA), or were based on a previous study (Peters *et al.*, 2007). The sequences of primer pairs are shown in Table 1.

Initial incubation at 95 °C for 10 s was followed by 40 PCR cycles consisting of denaturation at 95 °C for 5 s and annealing/elongation at 60 °C for 30 s. After the PCR reaction, final annealing was done for 15 s at 95 °C, followed by the melting curve reaction of gradual temperature increase from 60 to 90 °C.

Ct value was determined by the second derivative maximum method. Before the quantification of samples, standard curves of relative starting amount versus threshold cycles were drawn using pooled liver cDNA. The amplification efficiency of each reaction was within the range of 80 to 120%. The dissociation curve was confirmed to have single peak in each experiment. In addition, the PCR products were confirmed to be in agreement with their

theoretical sizes by agarose gel electrophoresis. The quantity of each transcript was determined by the relative amount of the mRNA to that of *RPL13A* by the ratio of mean Ct value. Relative quantity was also calculated using another house-keeping gene (*RPL32*) to confirm results. Data are presented here using *RPL13A* as the internal control gene.

#### Histopathological procedures

Paraffin-embedded liver specimens were sliced in 4- $\mu$ m thicknesses for hematoxylin and eosin (H & E) staining, Sirius red staining, and alpha-smooth muscle actin (alpha-SMA) immunohistochemistry according to a previously described procedure with minor changes (Junqueira *et al.*, 1979; Mekonnen *et al.*, 2007). For alpha-SMA immunostaining, antihuman SMA clone 1A4 antibody (Dako-Japan, Kyoto, Japan) at 1:200 dilution and Envision (goat anti-mouse, Dako-Japan) were used as primary and secondary antibodies, respectively. 3,3'-Diaminobenzidine (DAB, Dako-Japan) was used as the color substance. The reaction temperature and time for primary and secondary antibody and DAB was 4 °C overnight, room temperature for 30 min, and room temperature for 5 min, respectively. Slides were washed by phosphate buffered saline between each procedure, and skim milk was used as a blocking agent.

The degree of fibrosis in CH/LC was assessed semiquantitatively in 5 stages (0, absent; 1, mild with fibrous expansion of the portal area; 2, moderate; 3, severe, bridging

fibrosis; and 4, cirrhosis) with reference to stages of human liver disease. This quantitation has been applied to canine hepatitis (Shih *et al.*, 2007).

#### Clinical information

Clinical information including sex, age, and breed was obtained from medical records. The presence or absence of ascites and jaundice, which were identified as clinically prognostic factors in a multivariate analysis of a retrospective study (Poldervaart *et al.*, 2009), was also investigated.

#### Statistics for microarray experiment

After excluding unannotated genes and gathering probe set data that corresponded to the same gene, unsupervised hierarchical clustering was performed with the Pearson correlation coefficient as the measure of similarity and average linkage as the method to join clusters to see whether the whole gene expression profiles were different between the CONT, CH/LC, and ACSH groups.

To identify differentially expressed genes (DEGs) between any two of the three groups, analysis of variance was used with the  $P$  value set at 0.01, which corresponds to a false discovery rate of 6.3%. These genes were further analyzed by hierarchical clustering and visualized by heat map to classify genes according to the expression pattern among groups.

DEGs were divided into 6 clusters: cluster 1, ACSH > CH/LC and CONT; cluster 2, CH/LC and ACSH < CONT; cluster 3, ACSH and CONT > CH/LC; cluster 4, CH/LC > ACSH and CONT; cluster 5, ACSH > CH/LC and CONT; and cluster 6, CH/LC and ACSH > CONT. The significance of differences in expression of specific genes used for qPCR analysis was confirmed by the Rank Product method (Breitling *et al.*, 2004) using the R Bioconductor “RankProd” package with a false discovery rate < 5% considered significant.

Genes of each cluster were further analyzed by GENECODIS (Carmona-Saez *et al.*, 2007; Nogales-Cadenas *et al.*, 2009) to integrate gene lists into biological features with the KEGG pathway database. The data source (the list of reference genes and the annotations) for humans was used alternatively. A pathway was omitted if the number of DEGs in the pathway was < 5 or if the pathway was categorized in “Human diseases” or “Drug development”.  $P < 0.05$  was considered significant.

R and R bioconductor (<http://www.r-project.org/>), Microsoft Excel (Redmond, WA, USA), Cluster 2.0 (de Hoon *et al.*, 2004), and Java Treeview (Saldanha, 2004) were used for statistical analysis of microarray data.

#### Statistics for qPCR data

Comparisons of the expression levels of each gene between the three groups were done using the Steel-Dwass multiple comparison test. Correlations between transcript levels of

each gene and the degree of fibrosis were tested using Spearman's rank correlation test, and the differences of expression of each gene between dogs with and without poor prognostic clinical signs were tested using Mann-Whitney's U test. A  $P$ value  $< 0.05$  was considered significant. All statistical procedures were performed by R (<http://cran.r-project.org/>).

## Results

### Cases

Fifteen dogs were included in the CH/LC group. Ages ranged from 2 to 11 years. The breeds of the dogs included in this group were Labrador Retrievers (n = 6), Doberman Pinschers (n = 2), Yorkshire Terriers (n = 2), Shiba Inu (n = 1), Miniature Dachshund (n = 1), Chihuahua (n = 1), Irish Setter (n = 1), and American Cocker Spaniel (n = 1). One American Cocker Spaniel was classified in the CH/LC group because histologic findings did not show features of ACSH, especially spindle-shaped cell infiltration between degenerated hepatocytes. Dogs in the CH/LC group included two males, four females, two castrated males, and seven spayed females. The clinical signs of animals in the CH/LC groups included ascites (n = 6), jaundice (n = 5), lethargy (n = 4), and weight loss (n = 4). Copper concentration of liver tissue was determined in four of the six Labrador retrievers and both Doberman Pinschers, but none showed high copper accumulation consistent with copper-related hepatitis reported in these breeds (range: 77.2–616 µg/g dry weight).

Five American Cocker Spaniels were included in the ACSH group. They ranged in age from 2 to 6 years and included one male, two females, and two spayed females. Clinical signs in this group included ascites (n = 4), lethargy (n = 2), diarrhea (n = 2), vomiting (n = 1), and

weight loss (n = 1).

The age of beagle dogs (CONT group) ranged from 2 to 4 years. Three were spayed females and one was an intact male. No dog had any clinical signs, and screening serum biochemical tests, including alanine aminotransferase, alkaline phosphatase, serum urea nitrogen, and serum creatinine levels revealed no abnormalities.

#### Histopathological examination

The CH/LC group showed a wide range of inflammation and fibrosis on HE and Sirius red stains (Figure 14). Three cases were considered to be representative of cirrhosis (histologic stage 4 of fibrosis), that is, severe fibrosis, conversion of normal liver architecture, pseudolobules, or regenerative nodule formation. Lesions of mixed cell inflammation (macrophages, neutrophils, lymphocytes, and plasma cells), fibrosis, or hepatocyte degeneration were moderate to intermediate inside the lobular or pseudolobular areas, but these changes were severe in the peripheral or fibrotic areas of the cirrhotic liver.

Five cases showed severe fibrosis with fibrous tissue bridging (stage 3). In these cases, fibrosis was mostly seen near the portal areas. Inflammation was mainly seen around or inside the fibrous tissue, but was expanding to the lobular areas. Most of the inflammatory cells were lymphocytes, with minor infiltrations of macrophages and neutrophils. Hepatocytes were degenerating or were even necrotic adjacent to the lesions, and interface necrosis with some

apoptotic bodies was seen. Accumulation of red pigment, seemingly deposits of copper, was occasionally seen in the cytoplasm of hepatocytes.

Five cases were considered to have minimal ( $n = 2$ ) or moderate ( $n = 3$ ) fibrosis (stage 2). Inflammatory or degenerative findings were mild, and cell infiltration was limited to the portal areas. In the lobular areas, histologic changes were minimal.

Histologic findings of the ACSH group was different from those of the CH/LC group in all five cases. Intermediate to severe hepatocyte degeneration accompanied by prominent spindle-shaped cell infiltration was seen throughout the liver, and fibrosis was definite among mesenchymal cells. Architectural changes varied by case. In severe cases, regenerative nodules were also found, although these were not surrounded by the fibrous septa as seen in the CH/CL group. Inflammatory reactions were absent to moderate, and if present, were scattered all around the lobules. Cytoplasmic copper accumulation in hepatocytes was found occasionally.

#### Alpha SMA immunohistochemistry

On immunohistochemical analysis for alpha SMA in CONT samples, a positive reaction was noted around the portal area. Perisinusoidal lining cells were slightly positive for alpha SMA. Staining patterns were clearly different between the CH/LC and ACSH groups. In the CH/LC group, positive cells were distributed around the fibrous tissue (Figure 14). Spindle-shaped cells in the fibrous lesions showed cytoplasmic immunoreactivity for alpha

SMA. In addition, alpha SMA-positive cells were found all around the liver between hepatocytes in the ACSH group, corresponding to spindle-shaped cells abundantly observed in this group. Regenerative nodules found in some cases in the ACSH group had few alpha SMA-positive cells.

#### Microarray analysis

Clinical and histological findings of the cases examined are summarized in Table 5. Unsupervised hierarchical clustering distinguished the gene expression profiles of all three groups (Figure 15). Subsequently, DEGs between any two of the three groups were identified and clustered. A total of 2633 genes were considered DEGs and classified by hierarchical clustering (Figure 16). The DEGs and significantly relevant pathways are summarized in Table 6-1 to -6.

#### qPCR analysis of candidate genes for marker of liver fibrosis

Seven genes reportedly related to fibrosis were selected from genes up-regulated in the CH/LC group compared to the CONT group. To validate the difference of expression between groups, gene expression levels of these genes were compared between groups by qPCR (Figure 17). Expression levels of all the genes except for TGFB2 were significantly higher in CH/LC and ACSH groups compared to the control group ( $P < 0.05$ ) Gene expression levels did

not differ significantly between the CH/LC and ACSH groups ( $P < 0.05$ ).

#### Correlation between gene expression and histological degree of fibrosis in CH/LC

The relationship between the expression level of candidate genes and histologic degree of fibrosis in the CH/LC group is shown in Figure 18. CONT samples were included in this analysis as samples of stage 0 liver fibrosis. All expression levels were significantly correlated with the extent of histologic fibrosis ( $P < 0.01$ ,  $r > 0.6$ ). Using stepwise selection by Akaike's Information Criterion and multiple regression analysis showed that the expression levels of *PDGFD* and *THBS1* significantly predicted histologic degree of fibrosis with the standardized partial regression coefficients of 0.40 ( $P = 0.027$ ) and 0.54 ( $P = 0.005$ ), respectively, and the adjusted squared multiple correlation coefficient of 0.71. The overall  $P$  value in this model was 0.00002 (Table 3-3).

#### Expression levels of candidate genes in CH cases with and without negative prognostic signs

Comparisons of the expression of the candidate genes between CH/LF with and without ascites or jaundice (subgroup A and B, respectively) is shown in Figure 19. Subgroup A included nine cases (ascites only, 2; jaundice only, 1; ascites and jaundice, 4) and subgroup B, six cases. All expression levels were significantly ( $P < 0.05$ ) higher in subgroup A (with clinical signs) than in subgroup B (without clinical signs).

## Discussion

Gene expression analysis is a useful not only for obtaining basic information about a disease, but also for providing clinical and diagnostic information. Global expression analysis enables us to see an overview of the disease state, leading to the classification of disease subtypes and to identify genes that are related to the disease state. Quantification of mRNA of such genes can be a valuable diagnostic tool, because it is objective, reproducible, and quantitative (Sandvik *et al*, 2006).

Cirrhosis, the terminal stage of liver disease, is reported to be a negative prognostic factor in canine primary hepatitis (Poldervaart *et al*, 2009). Thus, it is an important role of diagnostic tools to predict how far the disease has progressed; this progression can be determined by estimating the degree of fibrosis. However, even though biopsy specimens can be taken and histopathologic examinations performed, the information obtained is subjective and qualitative, rather than quantitative.

To conquer this problem, I performed a microarray analysis using samples of diffuse parenchymal liver disease in dogs to identify candidate genes related to liver fibrosis and to show differences between CH/LC and ACSH. Subsequently, qPCR analysis was done to evaluate these genes as markers of fibrosis.

The microarray experiment showed that the whole transcriptional profile of CH/LC,

ACSH, and CONT samples were different. This result, in addition to clinical and histologic aspects previously described (Sakai, 2007), supports the concept of ACSH as a subtype of canine liver parenchymal disease. It is clinically important to understand this difference, because clinical outcome and even effective treatment can be different. In fact, it has been suggested that some cases of ACSH with severe clinical signs could recover (Sakai, 2007). This seems different from CH, in which cases with signs related to hepatic failure follow a rapid clinical course and have poor prognosis (Raffan *et al*, 2009). Furthermore, immunosuppressive therapy, the treatment of choice in CH (Favier, 2009), may not be effective in ACSH, because of the lack of severe immunological response. The difference in gene expression between CH/LC and ACSH helps explain the features and pathogenesis of ACSH and provides useful information to develop specific treatment.

The DEGs in both CH/LC and ACSH compared to the CONT group (Cluster 6 in the present study) were related to focal adhesion, extracellular matrix-receptor interaction, transforming growth factor-beta signaling, actin cytoskeleton, and proline metabolism, all of which are important for liver fibrosis. These results suggest that hepatic fibrosis occurs both in CH and ACSH, although the underlying mechanism seems to be different. In canine idiopathic CH, as well as in humans and experimental animals (Bataller and Brenner, 2005; Friedman, 2008), persistent inflammatory cell infiltration and subsequent hepatocyte necrosis and apoptosis trigger a fibroproliferative response. This concept was confirmed by the present study

in which the pathways related to natural killer cells, B and T lymphocytes, and cytokine interactions were upregulated in CH/LC. In contrast, such pathways were not upregulated in ACSH, suggesting that factors other than an inflammatory reaction induce a fibrogenic response in ACSH.

This idea is also supported by the results of immunohistochemistry for alpha SMA. Positive cells for alpha SMA were distributed all around the liver in ACSH; in contrast, in CH/LC, positive cells were mostly seen at the site of severe inflammation, hepatic injury, and fibrotic septa. Alpha SMA is a marker of activated hepatic stellate cells (HSC) or myofibroblasts (Ide *et al.*, 2001; Ijzer *et al.*, 2006). Immunohistochemistry results in the ACSH group indicate that factors stimulating the activation of HSC occur all around the liver. Factors other than inflammation have been reported to evoke activation of HSC and fibrosis (Friedman, 2008), but to my knowledge, nothing has been reported to cause histological changes in the liver as seen in ACSH. Because of the breed specificity, it is likely that genetic causes elicit HSC activation directly or indirectly in ACSH.

In the latter part of the present study, I performed a quantitative gene expression analysis of genes related to fibrosis derived from results of the microarray study. Furthermore, gene expression levels were compared to histological degree of fibrosis in the CH/LC group. Results related to these candidate genes in the microarray analysis were confirmed by qPCR and were similar to the microarray analysis, except for the failure to detect significant

upregulation of *TGFB2* expression in the CH/LC and ACSH groups compared to the CONT group. This discrepancy between results may be explained by differences in the quantification mechanism or insufficient sample sizes. When comparing the expressions of these genes with the extent of liver fibrosis on histopathology, mRNA quantity of all genes examined was well correlated with the degree of fibrosis, indicating the possibility that these genes may serve as markers of fibrosis. By selecting genes using Akaike's Information Criterion and multiple regression analysis, expression of two genes, namely *PDGFD* and *THBS1*, accurately predicted histologic fibrosis. A significant ( $P < 0.05$ ) difference in expression levels of candidate genes between cases with poor prognostic factors and those without them was also shown, supporting the idea that these results were clinically relevant.

*THBS1* is a family member of thrombospondins, which are multimeric, multidomain glycoproteins that function at cell surfaces and in the extracellular matrix. These gene products have been shown to be involved in wound healing, inflammatory reactions, and angiogenesis (Adams, 2001; Bornstein, 2001). *THBS1* transcript levels or protein levels have been shown to increase in hepatic fibrosis in humans (Paradis *et al.*, 2005) and experimentally induced cirrhosis in rats (Elpek *et al.*, 2008). *THBS1* plays a role in hepatic fibrosis through activating transforming growth factor-beta and the subsequent signal transduction with the regulation of Platelet derived growth factor (PDGF)-BB (Breitkopf *et al.*, 2005).

*PDGF-D* is a member of the PDGF family, a group of growth factors involved in

embryonic development, cell proliferation, and cell migration and angiogenesis in the form of homo- or heterodimers with another member of the PDGF family (Andrae *et al.*, 2008). Of the four members of PDGF family, PDGF-B and -D (Borkham-Kamphorst *et al.*, 2007) were reported to play an important role in hepatic fibrosis through the induction of HSC proliferation via binding to the PDGF receptor beta.

ACSH samples were not included in the study of the correlation between gene expressions and histology, because in ACSH, the pattern of fibrosis is so different that it seemed almost impossible to compare the extent of fibrosis with cases of CH/LC. However, because these marker genes were also upregulated in ACSH, this method can be used to determine the extent of fibrosis in ACSH.

This study has several limitations. First, the number of cases included in the present study and used for microarray analysis was small. This disadvantage raises a concern that cases included were not the representative of all cases. Second, because of the sample size and the lack of long time observation of clinical course, the clinical usefulness of these results is not clear. To address this limitation, expression levels between cases with clinical signs, which are related to worse prognosis, were compared to those without clinical signs.

In conclusion, I showed different gene expression levels between CH/LC and ACSH, a relatively new entity of canine liver disease. Furthermore, based on the findings of the microarray analysis, I proposed a simple, objective, and quantitative method for estimating the degree of

liver fibrosis using marker genes. In the future, results of this study can be used to help determine prognosis or be applied to the development of less invasive diagnostic tools such as serum markers or gene expression analysis using fine needle aspiration samples.

## **Conclusion**

Although there are various diagnostic examinations in canine liver disease, these have problems with diagnostic accuracy and objectivity. Among them, liver biopsy and subsequent histopathological examination, which is the gold standard of most of the liver diseases, have problems with not only the subjectivity but also the invasiveness. In this thesis, I attempted to develop novel diagnostic approaches to canine liver diseases which can compensate these problems around biopsy and histopathological examination.

In chapter 1, the enhancement pattern of liver in dogs and its diagnostic usefulness especially in the parenchymal phase in contrast-enhanced ultrasound using Sonazoid were shown. The important contribution of this result to veterinary clinical medicine is that clinicians can obtain the crucial information, i.e. the malignancy of the lesion, from ultrasonographic examination without anesthesia. No other agents have been reported to have a long contrast effect equivalent to Sonazoid in canine liver, and the enhancement duration of Sonazoid enables us to examine most of the dogs, which tend to move and do not suit for contrast-enhanced ultrasound examination using other agents with short enhancement effect duration. Because benign lesions frequently occur in older dogs, these lesions can be found incidentally during screening examination. Clinicians and owners hesitate to confirm them as benign ones by biopsy and histopathology because of its invasiveness. Contrast-enhanced ultrasound using Sonazoid can be a good option in that situation. On the other hand, Sonazoid was shown to have the potential to find lesions which are difficult to detect by conventional

ultrasound. It can be also used to examine whether dogs with primary malignancy outside or inside the liver have metastasis, which is the pivotal information for further examination or the choice of treatment. In future, it is needed to investigate the enhancement effect of Sonazoid in tumors which did not included in this study, for example, hepatocellular adenoma, hemangiosarcoma, or carcinoid.

In chapter 2, the usefulness of hyaluronan as a marker for liver cirrhosis in dogs and its possibility of a marker for liver fibrosis were shown. Hyaluronan can be a diagnostic aid for the clinical diagnosis in dogs with liver cirrhosis, which is often difficult to perform liver biopsy because of the bleeding risk or the presence of ascites. Furthermore, it can be possible to use hyaluronan in order to monitor the progression of liver disease to liver cirrhosis, which enables the evaluation of treatment efficacy. Considering the fact that most of the treatment for liver disease is empirical or based on poor evidence, it may help to develop better treatment in canine liver disease.

In Chapter 3, attempts to apply gene expression analysis for diagnostic test in canine parenchymal liver disease were conducted. First, microarray analysis revealed the difference of gene expression profile between chronic hepatitis (CH) and American Cocker Spaniel hepatopathy (ACSH), a newly proposed canine liver disease, supporting the concept that ACSH has different pathophysiological condition from CH. The gene expression profile of ACSH determined by reflected the presence of fibrogenic process and lack of severe inflammation.

Genes specifically up or down regulated in ACSH were also identified, but the evaluation of the importance of each gene was beyond the scope of this thesis. In future, further study is needed to show which genes are important in the pathogenesis of ACSH. Second, the candidate genes were extracted from the result of microarray experiment and the gene expression levels and the histological degree of fibrosis using CH samples were compared. Expression of all the genes examined was increased in accordance with the histological severity of fibrosis, and multivariate analysis showed that the combination of the expression levels of two genes, namely *PDGFD* and *THBS1*, explained the degree of fibrosis very well, suggesting that the quantification of these genes can be used as an objective scoring of fibrosis in canine chronic hepatitis. These results can also be applied to the development of noninvasive test such as blood marker of liver fibrosis or quantification of gene expression using samples obtained by fine needle aspiration in future.

The studies described here were limited to the preclinical study. To provide clinically important information by the methods suggested here, direct comparison of the results of the examinations and the clinical outcome such as prognoses or responses to treatment is needed in future.

In conclusion, I proposed a series of novel clinical examination methods, i.e. contrast-enhanced ultrasound using Sonazoid for neoplastic disorder, determining plasma hyaluronate concentration as a marker of cirrhosis, and gene expression analysis for chronic

parenchymal liver disorders in dogs. Using the new diagnostic methods developed here, I hope that the owner of the dogs with liver disease and clinical hepatologists can obtain better and more objective information than previous methods, leading to better diagnosis and treatment.

## Acknowledgement

I would like to express my deepest gratitude to Dr. Koichi Ohno for great support and advice during this study. I also would like to express my profound gratitude to Drs. Hajime Tsujimoto, Ryohei Nishimura, Kazuyuki Uchida, Yasuhito Fujino, Manabu Sakai, Yuko Goto - Koshino, Ko Nakashima and Masashi Takahashi for support of my works. I would like to acknowledge the substantial help from Drs. Kenjiro Fukushima and Mayumi Nakajima, Mr. Hirota Tomiyasu, and technical support from Drs. Koji Kadota and Yasuko Nakano.

I wish to thank all the patients and their owners in my works and all the staffs in Veterinary Medical Center of the University of Tokyo and the Department of Veterinary Internal Medicine.

Finally, I am most grateful to my family, Mr. Mitsuo Kanemoto, Mrs. Sumiko Kanemoto, Mr. Yasuyuki Kanemoto and Mr. Toshiyuki Kanemoto, to help me at all times.

## References

- Adams, J.C., 2001, Thrombospondins: multifunctional regulators of cell interactions. *Annu Rev Cell Dev Biol* 17, 25-51.
- Andrae, J., Gallini, R., Betsholtz, C., 2008, Role of platelet-derived growth factors in physiology and medicine. *Genes Dev* 22, 1276-1312.
- Arican, M., Carter, S.D., Bennett, D., 1996, Osteocalcin in canine joint diseases. *Br. Vet. J.* 152, 411-423.
- Arican, M., Carter, S.D., May, C., Bennett, D., 1994, Hyaluronan in canine arthropathies. *J. Comp. Pathol.* 111, 185-195.
- Balkman, C., 2009, Hepatobiliary neoplasia in dogs and cats. *Vet Clin North Am Small Anim Pract* 39, 617-625.
- Battaller, R., Brenner, D.A., 2005, Liver fibrosis. *J Clin Invest* 115, 209-218.
- Billir, D.S., Kantrowitz, B., Miyabayashi, T., 1992, Ultrasonography of diffuse liver disease. A review. *J Vet Intern Med* 6, 71-76.
- Bolondi, L., Correas, J.M., Lencioni, R., Weskott, H.P., Piscaglia, F., 2007, New perspectives for the use of contrast-enhanced liver ultrasound in clinical practice. *Dig Liver Dis* 39, 187-195.
- Borkham-Kamphorst, E., van Roeyen, C.R., Ostendorf, T., Floege, J., Gressner, A.M., Weiskirchen, R., 2007, Pro-fibrogenic potential of PDGF-D in liver fibrosis. *J Hepatol* 46, 1064-1074.
- Bornstein, P., 2001, Thrombospondins as matricellular modulators of cell function. *J Clin Invest* 107, 929-934.
- Bramigan, M., Burns, P.N., Wilson, S.R., 2004, Blood flow patterns in focal liver lesions at microbubble-enhanced US. *Radiographics* 24, 921-935.
- Breitkopf, K., Sawitza, I., Westhoff, J.H., Wickert, L., Dooley, S., Gressner, A.M., 2005, Thrombospondin 1 acts as a strong promoter of transforming growth factor beta effects via two distinct mechanisms in hepatic stellate cells. *Gut* 54, 673-681.
- Breitling, R., Armengaud, P., Amtmann, A., Herzyk, P., 2004, Rank products: a simple, yet powerful, new method to detect differentially regulated genes in replicated microarray experiments. *FEBS Lett* 573, 83-92.
- Budsberg, S.C., Lenz, M.E., Thonar, E.J., 2006, Serum and synovial fluid concentrations of keratan sulfate and hyaluronan in dogs with induced stifle joint osteoarthritis following cranial cruciate ligament transection. *Am. J. Vet. Res.* 67, 429-432.
- Camona-Saez, P., Chagoyen, M., Tirado, F., Carazo, J.M., Pascual-Montano, A., 2007, GENECODIS: a web-based tool for finding significant concurrent annotations in gene lists. *Genome Biol* 8, R3.
- Catala, V., Nicolau, C., Vilana, R., Pages, M., Bianchi, L., Sanchez, M., Bru, C., 2007,

- Characterization of focal liver lesions: comparative study of contrast-enhanced ultrasound versus spiral computed tomography. *Eur Radiol* 17, 1066-1073.
- Catalano, O., Nunziata, A., Lobianco, R., Siani, A., 2005, Real-time harmonic contrast material-specific US of focal liver lesions. *Radiographics* 25, 333-349.
- Center, S.A., 2007, Interpretation of liver enzymes. *Vet Clin North Am Small Anim Pract* 37, 297-333, vii.
- Chichibu, K., Matsuura, T., Shichijo, S., Yokoyama, M.M., 1989, Assay of serum hyaluronic acid in clinical application. *Clin. Chim. Acta* 181, 317-323.
- Cosgrove, D., Blomley, M., 2004, Liver tumors: evaluation with contrast-enhanced ultrasound. *Abdom Imaging* 29, 446-454.
- Cullen, J.M., 2009, Summary of the world small animal veterinary association standardization committee guide to classification of liver disease in dogs and cats. *Vet Clin North Am Small Anim Pract* 39, 395-418.
- Dai, Y., Chen, M.H., Yin, S.S., Yan, K., Fan, Z.H., Wu, W., Wang, Y.B., Yang, W., 2007, Focal liver lesions: can SonoVue-enhanced ultrasound be used to differentiate malignant from benign lesions? *Invest Radiol* 42, 596-603.
- de Hoon, M.J., Imoto, S., Nolan, J., Miyano, S., 2004, Open source clustering software. *Bioinformatics* 20, 1453-1454.
- Dietrich, C.F., 2004, Characterisation of focal liver lesions with contrast enhanced ultrasonography. *Eur J Radiol* 51 Suppl, S9-17.
- Elpek, G.O., Gokhan, G.A., Bozova, S., 2008, Thrombospondin-1 expression correlates with angiogenesis in experimental cirrhosis. *World J Gastroenterol* 14, 2213-2217.
- Favier, R.P., 2009, Idiopathic hepatitis and cirrhosis in dogs. *Vet Clin North Am Small Anim Pract* 39, 481-488.
- Feeney, D.A., Anderson, K.L., Ziegler, L.E., Jessen, C.R., Daubs, B.M., Hardy, R.M., 2008, Statistical relevance of ultrasonographic criteria in the assessment of diffuse liver disease in dogs and cats. *Am J Vet Res* 69, 212-221.
- Friedman, S.L., 2008, Mechanisms of hepatic fibrogenesis. *Gastroenterology* 134, 1655-1669.
- Gaschen, L., 2009, Update on hepatobiliary imaging. *Vet Clin North Am Small Anim Pract* 39, 439-467.
- Gomaa, A.I., Khan, S.A., Leen, E.L., Waked, I., Taylor-Robinson, S.D., 2009, Diagnosis of hepatocellular carcinoma. *World J Gastroenterol* 15, 1301-1314.
- Gressner, A.M., Haarmann, R., 1988, Hyaluronic acid synthesis and secretion by rat liver fat storing cells (perisinusoidal lipocytes) in culture. *Biochem. Biophys. Res. Commun.* 151, 222-229.
- Gressner, O.A., Weiskirchen, R., Gressner, A.M., 2007, Biomarkers of hepatic fibrosis, fibrogenesis and genetic pre-disposition pending between fiction and reality. *J. Cell Mol. Med.* 11, 1031-1051.
- Guehot, J., Laudat, A., Loria, A., Serfaty, L., Poupon, R., Giboudeau, J., 1996, Diagnostic accuracy of

- hyaluronan and type III procollagen amino-terminal peptide serum assays as markers of liver fibrosis in chronic viral hepatitis C evaluated by ROC curve analysis. *Clin. Chem.* 42, 558-563.
- Hall, R.L., 1985, Laboratory evaluation of liver disease. *Vet Clin North Am Small Anim Pract* 15, 3-19.
- Hohmann, J., Albrecht, T., Hoffmann, C.W., Wolf, K.J., 2003, Ultrasonographic detection of focal liver lesions: increased sensitivity and specificity with microbubble contrast agents. *Eur J Radiol* 46, 147-159.
- Ichida, T., Sugitani, S., Satoh, T., Matsuda, Y., Sugiyama, M., Yonekura, K., Ishikawa, T., Asakura, H., 1996, Localization of hyaluronan in human liver sinusoids: a histochemical study using hyaluronan-binding protein. *Liver* 16, 365-371.
- Ide, M., Yamate, J., Kuwamura, M., Kotani, T., Sakuma, S., Takeya, M., 2001, Immunohistochemical analysis of macrophages and myofibroblasts appearing in hepatic and renal fibrosis of dogs. *J Comp Pathol* 124, 60-69.
- Ijzer, J., Roskams, T., Molenbeek, R.F., Ultee, T., Penning, L.C., Rothuizen, J., van den Ingh, T.S., 2006, Morphological characterisation of portal myofibroblasts and hepatic stellate cells in the normal dog liver. *Comp Hepatol* 5, 7.
- Jang H.J., Kim, T.K., Burns, P.N., Wilson, S.R., 2007, Enhancement patterns of hepatocellular carcinoma at contrast-enhanced US: comparison with histologic differentiation. *Radiology* 244, 898-906.
- Junqueira, L.C., Bignolas, G., Brentani, R.R., 1979, Picrosirius staining plus polarization microscopy, a specific method for collagen detection in tissue sections. *Histochem J* 11, 447-455.
- Kim, T.K., Choi, B.I., Han, J.K., Hong H.S., Park, S.H., Moon, S.G., 2000, Hepatic tumors: contrast agent enhancement patterns with pulse-inversion harmonic US. *Radiology* 216, 411-417.
- Konopke, R., Bunk, A., Kersting S., 2007, The role of contrast-enhanced ultrasound for focal liver lesion detection: an overview. *Ultrasound Med Biol* 33, 1515-1526.
- Kudo, M., 2007, New sonographic techniques for the diagnosis and treatment of hepatocellular carcinoma. *Hepatol Res* 37 Suppl 2, S193-199.
- Kutara, K., Asano, K., Kito, A., Teshima, K., Kato, Y., Sasaki, Y., Edamura, K., Shibuya, H., Sato, T., Hasegawa, A., Tanaka, S., 2006, Contrast harmonic imaging of canine hepatic tumors. *J Vet Med Sci* 68, 433-438.
- Liptak, J.M., Withrow, S. J. , 2007, Cancer of the Gastrointestinal Tract, In: Withrow, S.J. (Ed.) WITHROW AND MACHEWENS SMALL ANIMAL CLINICAL ONCOLOGY. SAUNDERS ELSEVIER, St Louis, pp. 455 - 510.
- Manning D.S., Afzal, N.H., 2008, Diagnosis and quantitation of fibrosis. *Gastroenterology* 134, 1670-1681.
- Mekonnen, G.A., Ijzer, J., Nederbragt, H., 2007, Tenascin-C in chronic canine hepatitis: immunohistochemical localization and correlation with necro-inflammatory activity, fibrotic

- stage, and expression of alpha-smooth muscle actin, cytokeratin 7, and CD3+ cells. *Vet Pathol* 44, 803-813.
- Migaleddu, V., Virgilio, G., Turilli, D., Conti, M., Campisi, G., Canu, N., Sirigu, D., Vincentelli, I., 2004, Characterization of focal liver lesions in real time using harmonic imaging with high mechanical index and contrast agent levovist. *AJR Am J Roentgenol* 182, 1505-1512.
- Nganvongpanit, K., Itthiarbha, A., Ong-Chai, S., Kongtawelet, P., 2008, Evaluation of serum chondroitin sulfate and hyaluronan: biomarkers for osteoarthritis in canine hip dysplasia. *J. vet. Sci.* 9, 317-325.
- Nicolau, C., Bru, C., 2004, Focal liver lesions: evaluation with contrast-enhanced ultrasonography. *Abdom Imaging* 29, 348-359.
- Nicolau, C., Vilana, R., Catala, V., Bianchi, L., Gilabert, R., Garcia, A., Bru, C., 2006, Importance of evaluating all vascular phases on contrast-enhanced sonography in the differentiation of benign from malignant focal liver lesions. *AJR Am J Roentgenol* 186, 158-167.
- Nogales-Cadenas, R., Carmona-Saez, P., Vazquez, M., Vicente, C., Yang, X., Tirado, F., Carazo, J.M., Pascual-Montano, A., 2009, GeneCodis: interpreting gene lists through enrichment analysis and integration of diverse biological information. *Nucleic Acids Res* 37, W317-322.
- Nyman, H.T., Kristensen, A.T., Kjelgaard-Hansen, M., McEvoy, F.J., 2005, Contrast-enhanced ultrasonography in normal canine liver. Evaluation of imaging and safety parameters. *Vet Radiol Ultrasound* 46, 243-250.
- O'Brien, R.T., 2007, Improved detection of metastatic hepatic hemangiosarcoma nodules with contrast ultrasound in three dogs. *Vet Radiol Ultrasound* 48, 146-148.
- O'Brien, R.T., Iani, M., Matheson, J., Delaney, F., Young, K., 2004, Contrast harmonic ultrasound of spontaneous liver nodules in 32 dogs. *Vet Radiol Ultrasound* 45, 547-553.
- Ohlerth, S., O'Brien R. T., 2007, Contrast ultrasound: General principles and veterinary clinical applications. *Vet J.*
- Paradis, V., Bieche, I., Dargere, D., Cazals-Hatem, D., Laurendeau, I., Saada, V., Belghiti, J., Bezeaud, A., Vidaud, M., Bedossa, P., Valla, D.C., 2005, Quantitative gene expression in Budd-Chiari syndrome: a molecular approach to the pathogenesis of the disease. *Gut* 54, 1776-1781.
- Pares, A., Deulofeu, R., Gimenez, A., Caballeria, L., Bruguera, M., Caballeria, J., Ballesta, A.M., Rodes, J., 1996, Serum hyaluronate reflects hepatic fibrogenesis in alcoholic liver disease and is useful as a marker of fibrosis. *Hepatology* 24, 1399-1403.
- Peters, I.R., Peeters, D., Helps, C.R., Day, M.J., 2007, Development and application of multiple internal reference (housekeeper) gene assays for accurate normalisation of canine gene expression studies. *Vet Immunol Immunopathol* 117, 55-66.
- Plebani, M., Giacomini, A., Floreani, A., Chiamonte, M., Soffiati, G., Naccarato, R., Burlina, A., 1990, Biochemical markers of hepatic fibrosis in primary biliary cirrhosis. *Ric. Clin. Lab.* 20, 269-274.

- Poldervaart, J.H., Favier, R.P., Penning, L.C., van den Ingh, T.S., Rothuizen, J., 2009, Primary hepatitis in dogs: a retrospective review (2002-2006). *J Vet Intern Med* 23, 72-80.
- Raffan, E., McCallum, A., Scase, T.J., Watson, P.J., 2009, Ascites is a negative prognostic indicator in chronic hepatitis in dogs. *J Vet Intern Med* 23, 63-66.
- Rothuizen, J., Twedt, D.C., 2009, Liver biopsy techniques. *Vet Clin North Am Small Anim Pract* 39, 469-480.
- Saito, H., Shimamura, A., 2003, Ratekkusu gyosyūho ni yoru hiaruonsan sokutei shiyaku "erupiasu HA" nokisoteki kento. *J. Anal. Bio-Sci* 26, 69.
- Sakai, M., Sakamoto, Y., Takemura, A., Harada, K., Takiyama, N., Koie, H., Uechi, M., 2007, ACVIM Forum Abstract. *J Vet Intern Med* 21, 559-670.
- Sakugawa, H., Nakayoshi, T., Kobashigawa, K., Yamashiro, T., Maeshiro, T., Miyagi, S., Shiroma, J., Toyama, A., Kinjo, F., Saito, A., 2005, Clinical usefulness of biochemical markers of liver fibrosis in patients with nonalcoholic fatty liver disease. *World J. Gastroenterol.* 11, 255-259.
- Saldanha, A.J., 2004, Java Treeview—extensible visualization of microarray data. *Bioinformatics* 20, 3246-3248.
- Salwei, R.M., O'Brien, R.T., Matheson, J.S., 2003, Use of contrast harmonic ultrasound for the diagnosis of congenital portosystemic shunts in three dogs. *Vet Radiol Ultrasound* 44, 301-305.
- Salwei, R.M., O'Brien, R.T., Matheson, J.S., 2005, Characterization of lymphomatous lymph nodes in dogs using contrast harmonic and Power Doppler ultrasound. *Vet Radiol Ultrasound* 46, 411-416.
- Sandvik, A.K., Alsberg, B.K., Norsett, K.G., Yadetie, F., Waldum, H.L., Laegreid, A., 2006, Gene expression analysis and clinical diagnosis. *Clin Chim Acta* 363, 157-164.
- Sevelius, E., 1995, Diagnosis and prognosis of chronic hepatitis and cirrhosis in dogs. *J Small Anim Pract* 36, 521-528.
- Shih, J.L., Keating, J.H., Freeman, L.M., Webster, C.R., 2007, Chronic hepatitis in Labrador Retrievers: clinical presentation and prognostic factors. *J Vet Intern Med* 21, 33-39.
- Suzuki, Y., Fujimoto, Y., Hosoki, Y., Suzuki, M., Sakurai, S., Ohhira, M., Saito, H., Kohgo, Y., 2003, Clinical utility of sequential imaging of hepatocellular carcinoma by contrast-enhanced power Doppler ultrasonography. *Eur J Radiol* 48, 214-219.
- Szatmari, V., Harkanyi, Z., Voros, K., 2003, A review of nonconventional ultrasound techniques and contrast-enhanced ultrasonography of noncardiac canine disorders. *Vet Radiol Ultrasound* 44, 380-391.
- Tamaki, S., Ueno, T., Torimura, T., Sata, M., Tanikawa, K., 1996, Evaluation of hyaluronic acid binding ability of hepatic sinusoidal endothelial cells in rats with liver cirrhosis. *Gastroenterology* 111, 1049-1057.
- Tanaka, S., Ioka, T., Oshikawa, O., Hamada, Y., Yoshioka, F., 2001, Dynamic sonography of hepatic tumors. *AJR Am J Roentgenol* 177, 799-805.

- Ueno, T., Inuzuka, S., Torimura, T., Tamaki, S., Koh, H., Kin, M., Minetoma, T., Kimura, Y., Ohira, H., Sata, M., et al., 1993, Serum hyaluronate reflects hepatic sinusoidal capillarization. *Gastroenterology* 105, 475-481.
- Venable, R.O., Stoker, A.M., Cook, C.R., Cockrell, M.K., Cook, J.L., 2008, Examination of synovial fluid hyaluronan quantity and quality in stifle joints of dogs with osteoarthritis. *Am. J. Vet. Res.* 69, 1569-1573.
- Watanabe, R., Matsumura, M., Chen, C.J., Kaneda, Y., Fujimaki, M., 2005, Characterization of tumor imaging with microbubble-based ultrasound contrast agent, sonazoid, in rabbit liver. *Biol Pharm Bull* 28, 972-977.
- Watanabe, R., Matsumura, M., Chen, C.J., Kaneda, Y., Ishihara, M., Fujimaki, M., 2003, Grayscale liver enhancement with Sonazoid (NC100100), a novel ultrasound contrast agent; detection of hepatic tumors in a rabbit model. *Biol Pharm Bull* 26, 1272-1277.
- Watanabe, R., Matsumura, M., Munemasa, T., Fujimaki, M., Suematsu, M., 2007, Mechanism of hepatic parenchyma-specific contrast of microbubble-based contrast agent for ultrasonography: microscopic studies in rat liver. *Invest Radiol* 42, 643-651.
- Watson, P.J., Bunch, S. E., 2009, Diagnostic tests for the Hepatobiliary System, In: Nelson RW, C.C. (Ed.) *Small Animal Internal Medicine*. MOSBY elsevier, St. Louis, pp. 485-606.
- Wrigley, R.H., 1985, Radiographic and ultrasonographic diagnosis of liver diseases in dogs and cats. *Vet Clin North Am Small Anim Pract* 15, 21-38.
- Xu, H.X., Liu, G.J., Lu, M.D., Xie, X.Y., Xu, Z.F., Zheng Y.L., Liang J.Y., 2006, Characterization of focal liver lesions using contrast-enhanced sonography with a low mechanical index mode and a sulfur hexafluoride-filled microbubble contrast agent. *J Clin Ultrasound* 34, 261-272.
- Yanagisawa, K., Moriyasu, F., Miyahara, T., Yuki, M., Iijima, H., 2007, Phagocytosis of ultrasound contrast agent microbubbles by Kupffer cells. *Ultrasound Med Biol* 33, 318-325.
- Zanna, G., Fondevila, D., Bardagi, M., Docampo, M.J., Bassols, A., Ferrer, L., 2008, Cutaneous mucinosis in sharpei dogs is due to hyaluronic acid deposition and is associated with high levels of hyaluronic acid in serum. *Vet. Dermatol.* 19, 314-318.
- Zawie, D.A., Gilbertson, S.R., 1985, Interpretation of canine liver biopsy. A clinician's perspective. *Vet Clin North Am Small Anim Pract* 15, 67-76.
- Ziegler, L.E., O'Brien, R.T., Waller, K.R., Zagzebski, J.A., 2003, Quantitative contrast harmonic ultrasound imaging of normal canine liver. *Vet Radiol Ultrasound* 44, 451-454.

Table 1 Histological types and conventional ultrasound appearance of canine focal liver lesions

Lesion	Mean Size (Range)(cm)	Type		Echogenicity				
		Solitary	Multiple	Hypo	Iso	Hyper	Mixed	Target
Malignancy								
HCC (n=6)	6.3(3.5-8)	6		1	1		4	
CC (n=3)	3.7(2-7)	2	1	1			1	1
HT (n=4)	3.3(2-6)	1	3	4				
SA (n=3)	4.4(0.5-10)	2	1	1			1	1
Benignancy								
HN (n=9)	0.9(0.5-4)	6	3	7	1	1		

HCC: hepatocellular carcinoma, CC: cholangiocellular carcinoma, HT: hematopoietic tumor including lymphoma, mast cell tumor, and malignant histiocytosis, SA: sarcoma, HN: hyperplastic nodule, Hypo: hypoechoic, Iso: isoechoic, Hyper: hyperechoic compared to the liver parenchyma.

Table 2 Histological type and findings in contrast-enhanced ultrasound using Sonazoid

	Number of Dogs								
	Arterial			Portal			Parenchymal		
	Hyper	Iso	Hypo	Hyper	Iso	Hypo	ND	ID	CD
HCC (n=6)	5		1	1	1	4		6	
CC (n=3)			2			2		1	2
HT (n=4)	0	2	2			4			4
SA (n=3)			3			3		1	2
HN (n=9)		5	3		4	4	8		1

HCC: hepatocellular carcinoma, CC: cholangiocellular carcinoma, HT: hematopoietic tumor including lymphoma, mast cell tumor, and malignant histiocytosis, SA: sarcoma, HN: hyperplastic nodule, Arterial: arterial phase, Portal: portal phase, Parenchymal: parenchymal phase, Hyper: hyperenhancement, Iso: isoenhancement, Hypo: hypoenhancement compared to the liver parenchyma, ND: no defect, ID: irregular defect, CD: clear defect. One dog with CC and one dog with HN were examined only in the parenchymal phase.

Table 3 Histological type and vascular pattern in the arterial phase in contrast-enhanced ultrasound using Sonazoid

	Number of Dogs						
	Dysmorphic	Radial	Diffuse		stippled	Peripheral	Hypoperfused
			Inhomogeneous	Homogeneous			
HCC (n=6)	4	1	1				
CC (n=2)					1	1	
HT (n=4)			1		1	2	
SA (n=3)			1	1		1	
HN (n=8)				6			2

HCC: hepatocellular carcinoma, CC: cholangiocellular carcinoma, HT: hematopoietic tumor including lymphoma, mast cell tumor, and malignant histiocytosis, SA: sarcoma, HN; hyperplastic nodule, Arterial: arterial phase, Portal: portal phase, Parenchymal: parenchymal phase

Table 4 Primer pairs

Gene Symbol	Forward primer	Reverse primer
<i>BAMBI</i>	ATCGCCATTCAGCTACATC	GGCAGCATCACAGTAGCATC
<i>COL1</i>	AAGAGCCTGAGCCAGCAGATC	AGTCGGAGTGGCACATCTTGA
<i>COL3</i>	GGCACAGCAGCAAGCTATTG	GGTTCTGGCTTCCAGACATCTC
<i>PDGFD</i>	AGGAACCTGCTGCTCACCT	CCACACCACCGTCCTCTAAT
<i>TGFB2</i>	GACCCACATCTCCTGCTAA	CACCCAAGATCCCTCTTGAA
<i>THBS1</i>	GAAGGATTCCGATGGTGATG	ATCTGCGGAAATCAGTCTCG
<i>TIMP1</i>	AAGTCAACCAGACCGACTTAAACC	TCCCAAGGCGCTGAAA
<i>RPL13A</i>	GCCGGAAGGTTGTAGTCGT	GGAGGAAGGCCAGGTAATTC
<i>RPL32</i>	TGGTTACAGGAGCAACAAGAAA	GCACATCAGCAGCACTTCA

Table 5 The clinical and histological findings of the cases used for microarray analysis

Case	Breed	Age (year)	Sex	Clinical signs	Survival time	Fibrosis/Severity
ACSH1	ACS	2	F	Ascites, vomiting	300 day (cencered)	mild
ACSH2	ACS	2	M	Ascites	3 years (cencered)	mild
ACSH3	ACS	5	SF	Ascites, jaundice, melena	63 days	severe
CH/LC1	LR	10	SF	Ascites, weight loss	200 days (cencered)	3
CH/LC2	LR	6	SF	Ascites	63 days	3
CH/LC3	DM	6	SF	Ascites, jaundice, weight loss	75 days	4
CONT1	BG	4	M	-	-	0
CONT2	BG	4	SF	-	-	0
CONT3	BG	2	M	-	-	0

ACSH: American Cocker Spaniel hepatopathy, CH/LC: Chronic hepatitis/ liver cirrhosis, CONT: control

F: female, M: male, SF: spayed female

In ACSH, the subjective severity of the histological change was written.

In CH/LC, the degree of fibrosis was classified into stage 0 to 4, according to the criteria as explained in the text.

Table 6-1 Pathways significantly related to the genes of cluster 1 (CH/LC and ACSH &gt; CONT)

<i>P</i> value	Description	Genes in this cluster
9.46E-16	Focal adhesion	<i>COL1A1, COL1A2, COL3A1, COL5A1, ITGA6, COL5A2, VWF, HGF, SPP1, FLNA, CAPN2, CAV1, CCND2, COL4A1, COL4A2, ITGB5, LAMA4, LAMB1, LAMC1, PAK2, MAP2K1, THBS1, THBS2, THBS4, VEGFC, RAP1B, LAMC2, PDGFD, MYLK, CCND1, MAPK10, SHC1, CAV2</i>
2.44E-12	ECM-receptor in teraction	<i>COL1A1, COL1A2, COL3A1, COL5A1, ITGA6, COL5A2, VWF, SPP1, COL4A1, COL4A2, ITGB5, LAMA4, LAMB1, LAMC1, THBS1, THBS2, THBS4, LAMC2, AGRN</i>
1.91E-10	Cell Communication	<i>COL1A1, COL1A2, COL3A1, COL5A1, ITGA6, COL5A2, VWF, SPP1, COL4A1, COL4A2, DES, LAMA4, LAMB1, LAMC1, THBS1, THBS2, THBS4, VIM, LAMC2, LMNA</i>
0.00028167	Cell cycle	<i>CCND2, E2F5, MAD2L1, TGFB2, CDC7, MCM6, YWHAQ, CDC2, CCND1, YWHAZ, PCNA</i>
0.00159099	Gap junction	<i>HTR2B, GNAI1, ITPR3, MAP2K1, NPR2, TUBA1A, TUBA1B, PDGFD, CDC2</i>
0.00244216	TGF-beta signaling pathway	<i>E2F5, TGFB2, THBS1, THBS2, THBS4, PPP2CB, DCN, ID1</i>
0.00267405	Regulation of actin cytoskeleton	<i>ITGA6, CD14, ITGB5, PAK2, MAP2K1, EZR, CFL1, ARPC3, ARPC1B, ARPC1A, ARPC5L, MYLK, ARPC2, GSN</i>
0.00398335	MAPK signaling pathway	<i>CACNB3, CD14, FLNA, HSPB2, MEF2C, PAK2, MAP2K1, TGFB2, DUSP14, RAP1B, MAPKSP1, CASP4, MAPK10, MAP4K4, MAX, STMN1</i>
0.02192154	Arginine and proline metabolism	<i>MAOA, GATM, LOXL2, SAT1, P4HA2</i>

Table 6-1 Continued

<i>P</i> value	Description	Genes in this cluster
0.04212971	Complement and coagulation cascades	<i>A2M, F13A1, VWF, CFD, PLAT</i>
0.04750516	Leukocyte transendothelial migration	<i>IL8, CTNND1, GNAI1, EZR, RAP1B, CLDN18, VCAM1</i>
0.04825051	Toll-like receptor signaling pathway	<i>IL8, CD14, TLR2, LBP, LY96, MAPK10</i>

Table 6-2 Pathways significantly related to the genes of cluster 2 (ACSH > CH/LC and CONT)

<i>P</i> value	Description	Genes in this cluster
0.00222323	Focal adhesion	<i>RHOA, CTNNB1, GNAI2, MYH9, CLDN5, RRAS</i>
0.00128022	Insulin signaling pathway	<i>FLOT2, RHEB, RRAS, CALM1, MAPK1, PRKAA1</i>
0.00057721	Tight junction	<i>RHOA, CTNNB1, GNAI2, MYH9, CLDN5, RRAS</i>
0.03532872	Regulation of actin cytoskeleton	<i>RHOA, F2R, MYH9, RRAS, MAPK1</i>
0.00341475	Leukocyte transendothelial migration	<i>PECAM1, RHOA, CTNNB1, GNAI2, CLDN5</i>

Table 6-3 Pathways significantly related to the genes of cluster 3 (CH/LC > ACSH and CONT)

<i>P</i> value	Description	Genes in this cluster
0.00751779	Natural killer cell mediated cytotoxicity	<i>ICAM2, CD48, PAK1, GZMB, LCK, NFAT5, TYROBP, GRB2, PRKCB</i>
0.0112933	Toll-like receptor signaling pathway	<i>IL1B, CXCL10, CCL4, CCL5, CD80, CD40, CD86</i>
0.01569101	Cytokine-cytokine receptor interaction	<i>IL2RG, IL1B, CCR5, IL10RB, CCR1, CXCL10, IL7R, CCL4, CCL5, TNFRSF14, LTB, CD40, CSF3R</i>
0.02173749	Cell adhesion molecules (CAMs)	<i>CCR5, ICAM2, ITGA4, ITGB7, CCR1, CD80, NLGN1, NRXN1, CD40, CSF3R, CD86</i>
0.02563161	Cell cycle	<i>ATR, BUB1B, CCNA2, PTTG1, CCNB2, CDKN2C, YWHAB</i>
0.02586907	Hematopoietic cell lineage	<i>IL1B, CD3E, ITGA4, IL7R, CD7, CSF3R</i>
0.03773017	B cell receptor signaling pathway	<i>BTK, LYN, CD81, NFAT5, PRKCB</i>
0.04601493	T cell receptor signaling pathway	<i>CD3E, PAK1, LCK, CBLB, NFAT5, GRB2</i>

Table 6-4 Pathways significantly related to the genes of cluster 4 (CH/LC < ACSH and CONT)

<i>P</i> -value	Description	Genes in this cluster
0.0000513	Valine, leucine and isoleucine degradation	<i>ACADM, MUT, HSD17B4, AUH, EHHADH, ECHS1, HADH, ALDH6A1, ACAT2</i>
0.00013903	Caprolactam degradation	<i>HSD17B4, EHHADH, ECHS1, HADH, SIRT2</i>
0.00020862	Fatty acid metabolism	<i>ACADM, HSD17B4, ADH1C, EHHADH, ECHS1, HADH, ACAT2, ACSL4</i>
0.00027287	Butanoate metabolism	<i>HSD17B4, EHHADH, ECHS1, HADH, ACAT2, ILVBL, L2HGDH, HSD3B7</i>
0.00030852	Complement and coagulation cascades	<i>CFI, PLG, C1QB, SERPINA5, SERPINA1, CFH, C1R, FGA, C1S</i>
0.00071746	SNARE interactions in vesicular transport	<i>STX7, VAMP8, SEC22B, VAMP7, VTI1B, SNAP23</i>
0.00224743	Arginine and proline metabolism	<i>OTC, CPS1, RARS, GLUD1, LOXLA, GAMT, ALDH4A1</i>
0.00329874	Lysine degradation	<i>HSD17B4, EHHADH, ECHS1, HADH, ACAT2, COPS5, HSD3B7</i>
0.00599112	Adipocytokine signaling pathway	<i>STK11, CD36, TNFRSF1A, AKT2, PRKAB1, ADIPOR1, ACSL4</i>
0.0061807	Tryptophan metabolism	<i>HSD17B4, AFMID, EHHADH, KYNU, ECHS1, HADH, ACAT2, TRAF7</i>
0.01152074	Starch and sucrose metabolism	<i>UGDH, UGP2, UGT2A1, TREH, GBA3, GYS2, SMARCA2</i>
0.0140894	Insulin signaling pathway	<i>AKT2, PTPN1, PRKAB1, RRAS2, GYS2, MAP2K2, PKLR, PKM2, PPP1CB, PRKACA</i>
0.02525291	Axon guidance	<i>MET, PAK4, GNAI3, RRAS2, RHOD, RAC1, NGEF, LRRC4C, CFL2</i>

Table 6-5 Pathways significantly related to the genes of cluster 5 (CH/LC and ACSH < CONT)

<i>P</i> value	Description	Genes in this cluster
0.00000629	Lysine degradation	<i>ALDH1B1, ALDH3A2, ALDH7A1, BBOX1, GCDH, HSD17B12, EHMT2, SHMT1, NAT5, AADAT</i>
0.0000756	Fatty acid metabolism	<i>ALDH1B1, CYP4A11, ALDH3A2, ALDH7A1, ACADL, ACOX1, GCDH, ADHFE1</i>
0.0000897	Citrate cycle (TCA cycle)	<i>PCK1, SDHB, SDHC, PCK2, IDH3B, ACLY</i>
0.00010775	Bile acid biosynthesis	<i>SRD5A2, ALDH1B1, ALDH3A2, ALDH7A1, CEL, HSD17B12, ADHFE1</i>
0.00011383	Valine, leucine and isoleucine degradation	<i>HMGCL, PCCB, ALDH1B1, ALDH3A2, ALDH7A1, ACADL, NAT5, BCKDHB</i>
0.00014733	Pyruvate metabolism	<i>ALDH1B1, ALDH3A2, ALDH7A1, PCK1, PCK2, ACSS2, ACOT12</i>
0.00060266	Propanoate metabolism	<i>PCCB, ALDH1B1, ALDH3A2, ALDH7A1, ACADL, ACSS2</i>
0.00062521	Butanoate metabolism	<i>HMGCL, ALDH1B1, ALDH3A2, ALDH7A1, HSD17B12, ALDH5A1, NAT5</i>
0.00072156	beta-Alanine metabolism	<i>ALDH1B1, ALDH3A2, ALDH7A1, ACADL, UPB1</i>
0.00138831	Limonene and pinene degradation	<i>ALDH1B1, ALDH3A2, ALDH7A1, NAT5, DHRS2</i>
0.00730753	Glycine, serine and threonine metabolism	<i>SARDH, HSD17B12, GNMT, SHMT1, CHKA</i>
0.00841952	Glycolysis / Gluconeogenesis	<i>ALDH1B1, ALDH3A2, ALDH7A1, PGM1, ACSS2, ADHFE1</i>
0.00957275	Tryptophan metabolism	<i>ALDH1B1, ALDH3A2, ALDH7A1, HAAO, GCDH, ACMSD, AADAT</i>
0.0133168	Histidine metabolism	<i>ALDH1B1, ALDH3A2, ALDH7A1, HNMT, NAT5</i>

Table 6-5 Continued

<i>P</i> value	Description	Genes in this cluster
0.01550626	Androgen and estrogen metabolism	<i>HSD17B3, SRD5A2, HSD17B7, HSD11B1, UGT1A6</i>
0.0250175	Tyrosine metabolism	<i>TAT, DBH, ADHFE1, GSTZ1, NAT5</i>
0.04631065	Metabolism of xenobiotics by cytochrome P450	<i>GSTA4, EPHX2, ADHFE1, GSTZ1, UGT1A6</i>

Table 6-6 Pathways significantly related to the genes of cluster 5 (ACSH < CH/LC and CONT)

<i>P</i> -value	Description	Genes in this cluster
0.01011	Neuroactive ligand-receptor interaction	<i>CCKAR, CRH, NPY2R, PRLR, TACR3, LEPR, DRD2, GABRG2, THRA</i>
0.015206	Focal adhesion	<i>COL4A4, IGF1, ITGB6, TNC, ITGA7, TTN, SHC4</i>
0.021237	Calcium signaling pathway	<i>PHKA2, CACNA1E, CCKAR, TACR3, TTN, PTK2B</i>

## Figure Legends

Figure 1. Schema of the enhancement pattern in the arterial phase. Radial enhancement (A), dysmorphic vascular enhancement (B), diffuse inhomogeneous enhancement (C), diffuse homogeneous enhancement (D), fine, stippled enhancement (E), peripheral enhancement (F), hypoenhancement (G)

Figure 2. Time course of mean gray-scale intensity of liver parenchyma (○) and liver portal vein (■). Time 0 corresponds to the time of Sonazoid injection.

Figure 3. Time course of mean gray-scale intensity of spleen (△) and renal cortex (×). Time 0 corresponds to the time of Sonazoid injection.

Figure 4. Sonographic image of one representative case of hepatocellular carcinoma (HCC) in the conventional B-mode ultrasound (A) and in the arterial (B), portal (C), and parenchymal (D) phases of Sonazoid CEU (contrast enhanced ultrasound). In the conventional B-mode ultrasound, a bulky focal lesion was observed inside the liver in the right side of the screen (A). In CEU, dysmorphic vessels with diffuse enhancement in the parenchyma of the lesion in the arterial phase (B), diffuse but irregular enhancement without

recognizable vascular shape in the portal phase (C), and weaker enhancement compared to the surrounding liver (left side) with irregular enhancement defect in the parenchymal phase (D) were observed.

Figure 5. Sonographic image of one representative case of cholangiocellular carcinoma (CC) in the conventional B-mode ultrasound (A) and in the arterial (B), portal (C), and parenchymal (D) phases of Sonazoid CEU (contrast-enhanced ultrasound). A hypoechoic, well-circumscribed focal lesion was observed on the visceral surface of the liver in the conventional B-mode ultrasound (A). In CEU, the nodule was hypovascular compared with the surrounding liver parenchyma, with fine feeding vessels flowing in and forming a dotted pattern (A) in the arterial phase; it was hypovascular in the portal phase (C); and it was clearly observed as a defect in the parenchymal phase (D).

Figure 6. Sonographic image of malignant histiocytosis in the conventional B-mode ultrasound (A), and in the arterial (B), portal (C), and parenchymal (D) phases of Sonazoid CEU (contrast-enhanced ultrasound). Multiple target lesions were observed in the conventional B-mode ultrasound images (A). In CEU, we observed hypovascularity with peripheral enhancement of the lesion in the arterial phase (B), early enhancement washout in the portal phase (C), and a defect with a target-like pattern and clear border (D) in the parenchymal phase.

Figure 7. Sonographic image of a sarcoma of unknown origin in the conventional B-mode ultrasound (A) and in the arterial (B), portal (C), and parenchymal (D) phases of Sonazoid CEU (contrast-enhanced ultrasound). In the conventional B-mode ultrasound, typical target lesions were observed diffusely in the liver. In CEU, hypovascularity inside lesions with peripheral enhancement of some nodules in the arterial phase (B), early enhancement washout and hypovascularity in the portal phase (C), and defect with a target-like pattern and clear border (D) in the parenchymal phase were observed.

Figure 8. Sonographic image of a nodular hyperplasia in the conventional B-mode ultrasound (A), and in the arterial (B), portal (C), and parenchymal (D) phases of Sonazoid CEU (contrast-enhanced ultrasound). In the conventional B-mode ultrasound, a solitary, ill-defined, hypovascular lesion was observed. In CEU, we observed isovascularity in the arterial (B), portal (C), and parenchymal phases and the lesion became unclear (C). No defects were observed inside the nodule.

Figure 9. Blood HA concentration in the 4 groups Group 0: healthy beagles; Group 1: dogs with chronic liver disease without cirrhosis; Group 2: dogs with cirrhosis; Group 3: dogs with extrahepatic disease. The blood HA concentrations were significantly higher in Group 2

than in Group 0, Group 1, and Group 3. Also, Group 2 had significantly higher HA concentration than and Group 3. \*  $P < 0.05$ .

Figure 10. Post-prandial serum total bile acid concentration in group 1 and 2. Group 1: dogs with chronic liver disease without cirrhosis, Group 2: dogs with cirrhosis. There is no statistical difference between two groups ( $P = 0.27$ ).

Figure 11. The relationship of histological degree of fibrosis and circulating HA concentration. The correlation was statistical but weak ( $P < 0.05$ ,  $r = 0.44$ ).

Figure 12. Blood HA levels of dogs with hepatitis. "Symptomatic" indicates dogs with clinical signs of ascites and/or jaundice, both of which are negative prognostic factor of hepatitis, and "asymptomatic" means dogs without these signs. The symptomatic dogs had significantly higher HA concentration than the asymptomatic dogs. ( $P < 0.01$ )

Figure 13. Histological distribution of HA in the liver: a, b, c, d: a healthy beagle; e, f, g, h: a dog with severe fibrosis without cirrhosis; i, j, k, l: a dog with cirrhosis. The stains used were as follows: first line (a, e, i): HE stain; second line (b, f, j): Sirius Red stain, collagen is stained in red; third line (c, g, k): histochemistry for HA; fourth line (d, h, l): negative control of HA. In

healthy livers, the portal area was only slightly stained for HA (depicted as brown in color, c). The liver with hepatitis and moderate to severe fibrosis showed staining around the portal areas in which the fibrosis was progressing (f, g). HA was detected in a part of the fibrotic septa in the cirrhotic liver (j, k). Bar=100µm

Figure 14. Histological and immunohistological finding of chronic hepatitis and American Cocker Spaniel hepatopathy. a, b, c: Chronic hepatitis, d,e,f,g,h: American Cocker Spaniel hepatopathy. The stains used were as follows: a, d, g: HE stain, b,e: Sirius red stain, c, f, h: Immunohistochemistry for alpha smooth muscle actin. The magnification was ×40 (a-f) and ×200 (g, h). In chronic hepatitis, inflammation, hepatocyte loss and fibrosis were seen mostly around the portal area, and the positive staining for alpha SMA corresponded to the fibrous tissue. This case had severe inflammation and bridging fibrosis, assigned to stage 3 fibrosis. In American Cocker Spaniel hepatopathy, severe hepatocyte degeneration, spindle-shaped cell infiltration, fibrosis and mild to moderate inflammation was seen all around the liver, although the architecture was severely distorted. A regenerative nodule without fibrotic septa was seen in this picture (\*). The positive cells for alpha smooth muscle actin were distributed all around the lobule and distributed between hepatocytes, forming mesh-like staining pattern.

Figure 15. Unsupervised clustering for gene expression profiles of nine samples. The

unsupervised clustering distinguished three groups (control group, American Cocker Spaniel hepatopathy group (ACSH), and chronic hepatitis/cirrhosis group (CH/LC)).

Figure 16. The result of hierarchical clustering of genes differentially expressed between any two of the three groups. 2623 genes were identified as differentially expressed genes.

Figure 17. The expression of candidate genes in control, chronic hepatitis, and American Cocker Spaniel hepatopathy. The result of the samples included in microarray analysis was shown in red cross, and others were expressed as black circle. \*,; Significant difference with  $P$  value less than 0.05.

Figure 18. The relationship between histological degree of fibrosis and the expression of candidate genes. The expression of all the genes was significantly ( $P < 0.005$ ) and strongly ( $r > 0.6$ ) correlated to the degree of fibrosis.<sup>6</sup>

Figure 19 The expression of candidate genes in chronic hepatitis with or without clinical signs related to poor prognosis i.e. icterusa and/or ascites. Expression of all the genes was significantly higher in cases with the clinical signs (subgroup B) than those without them (subgroup A).

Figure 1

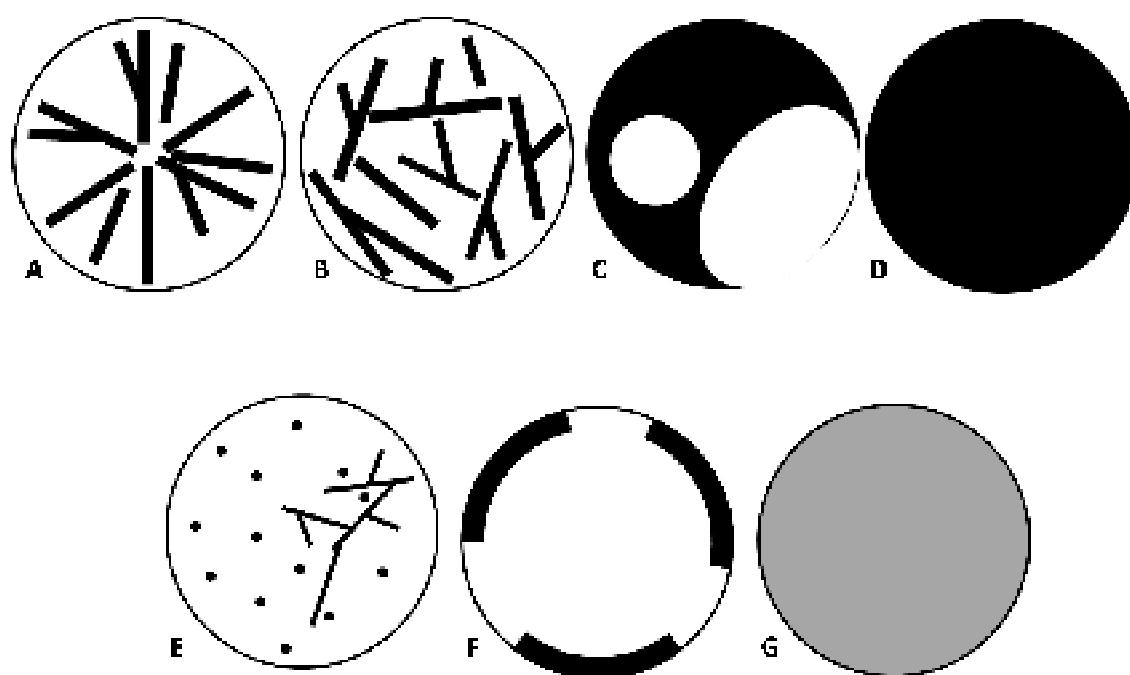


Figure 2

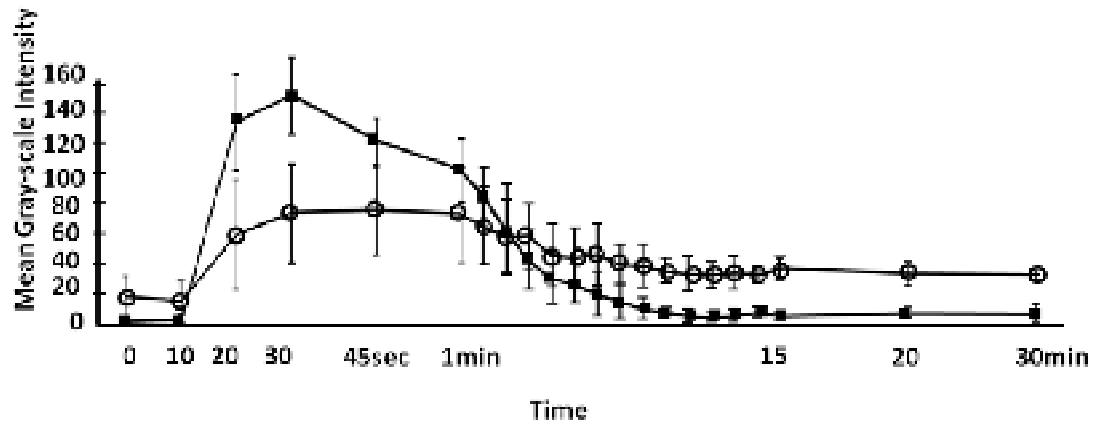


Figure 3

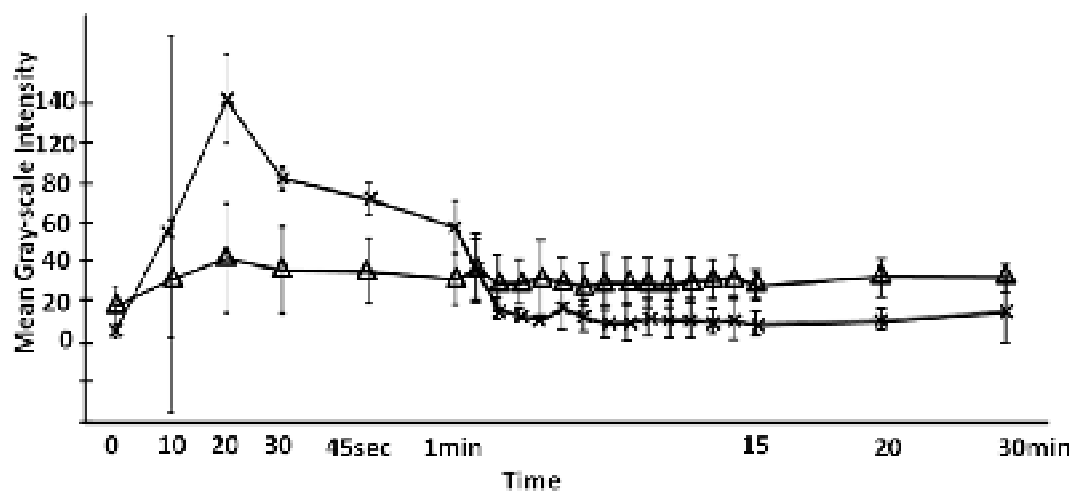


Figure 4

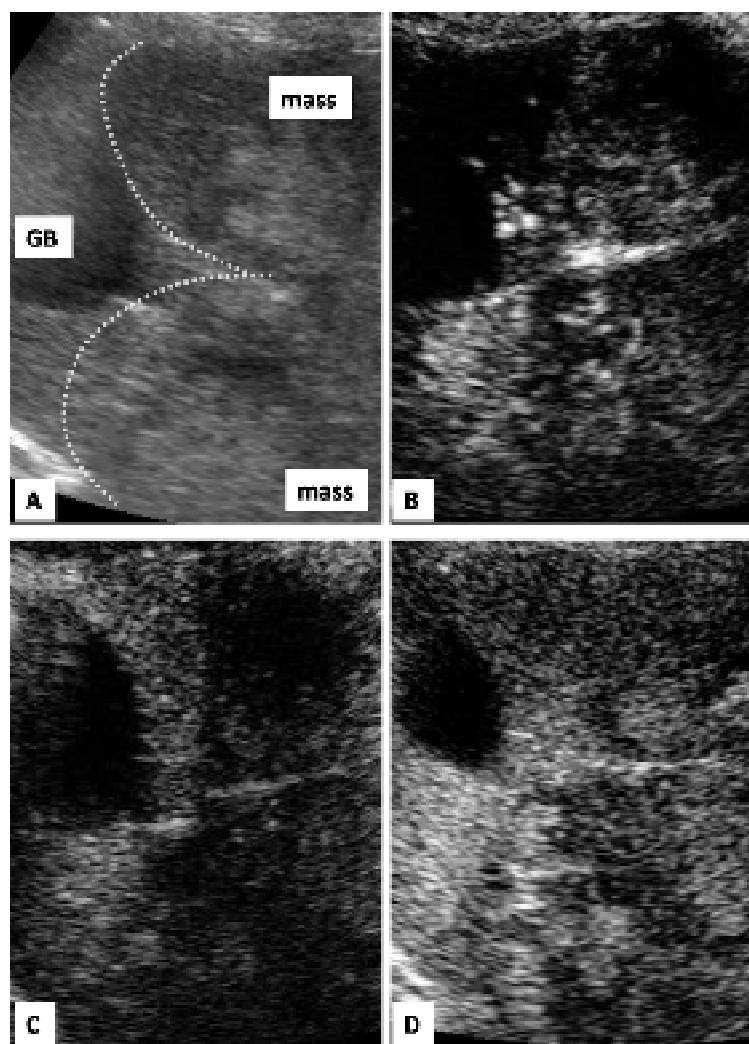


Figure 5

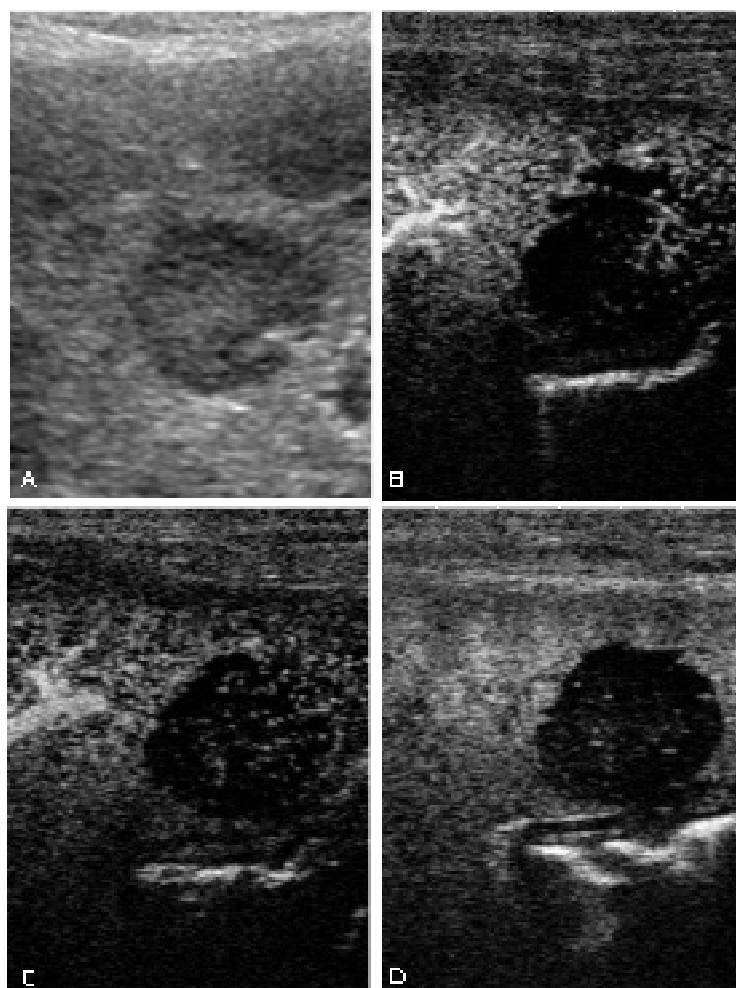


Figure 6

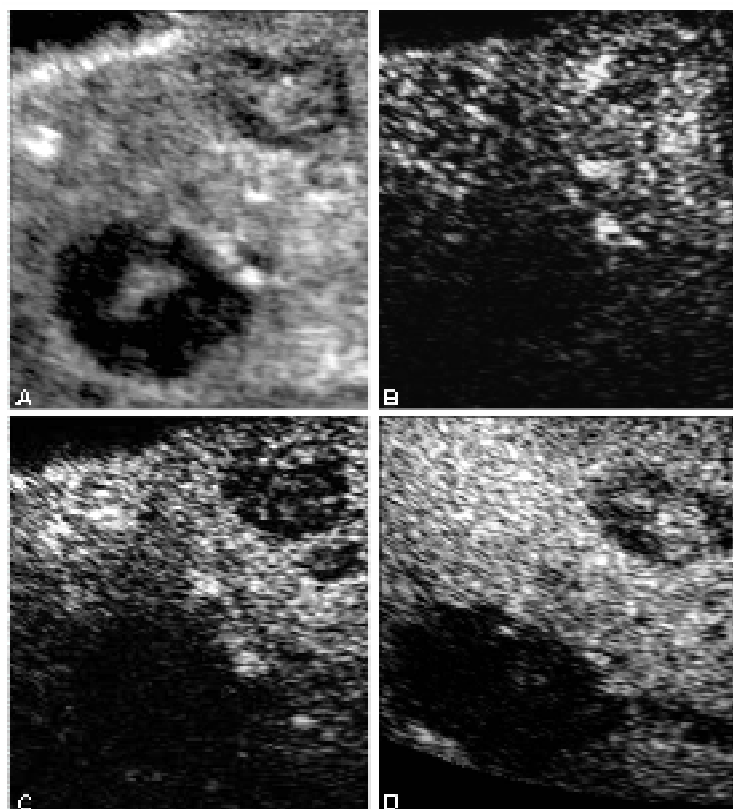


Figure 7

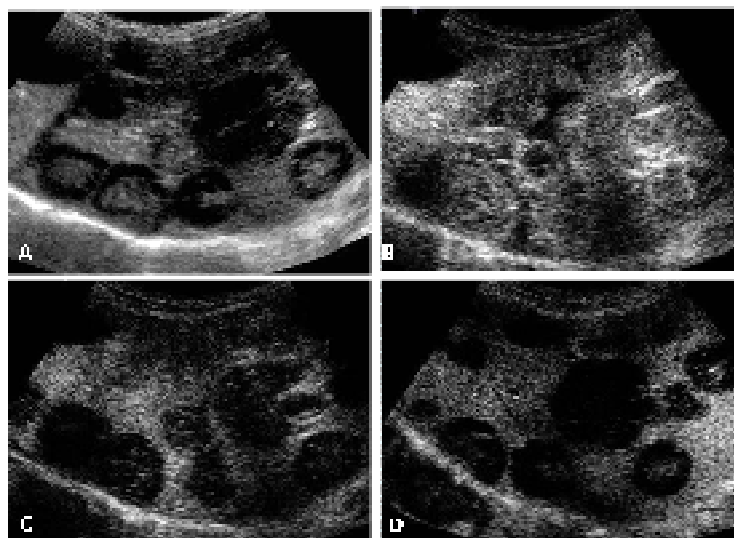


Figure 8

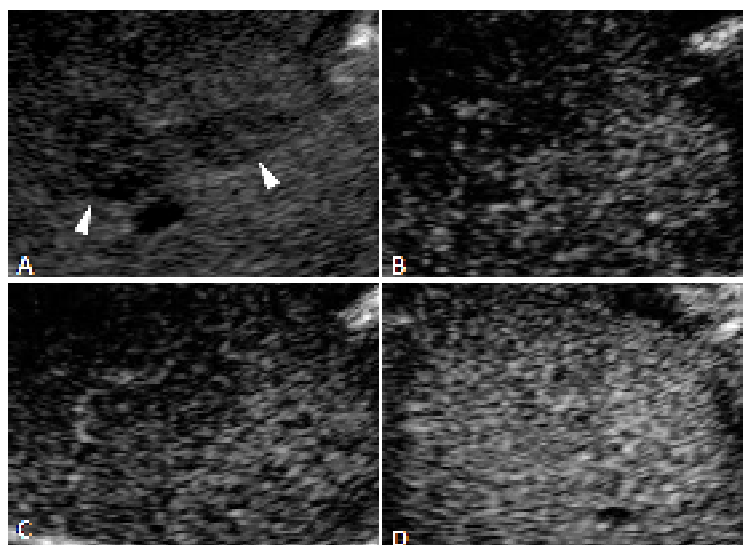


Figure 9

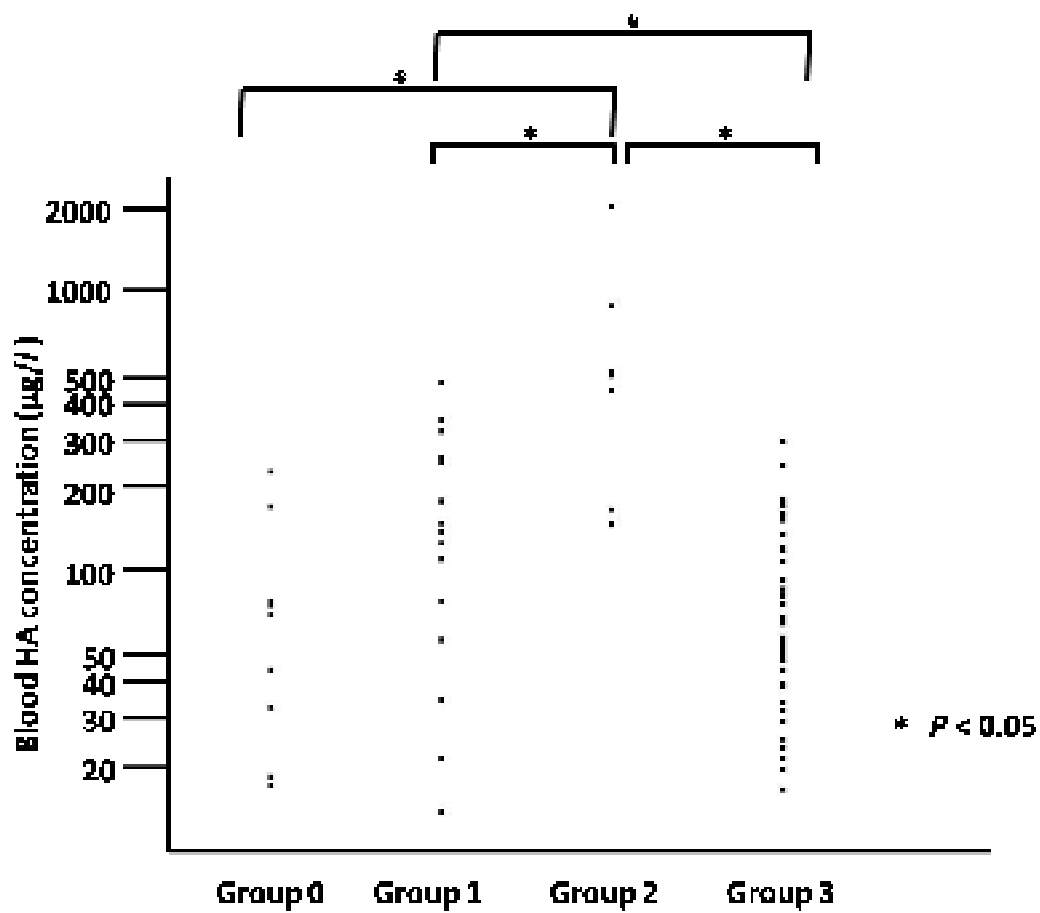


Figure 10

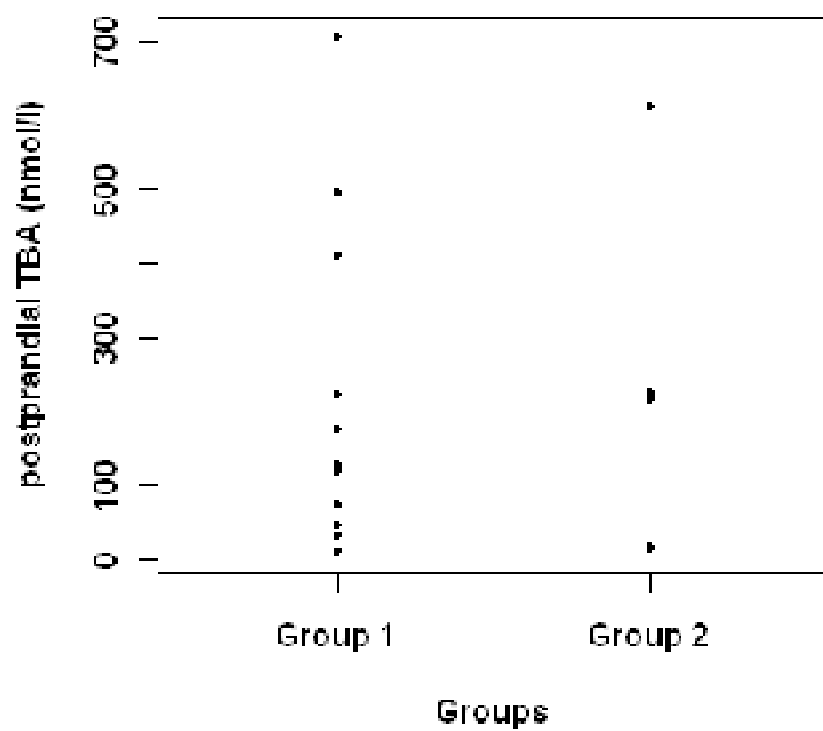


Figure 11

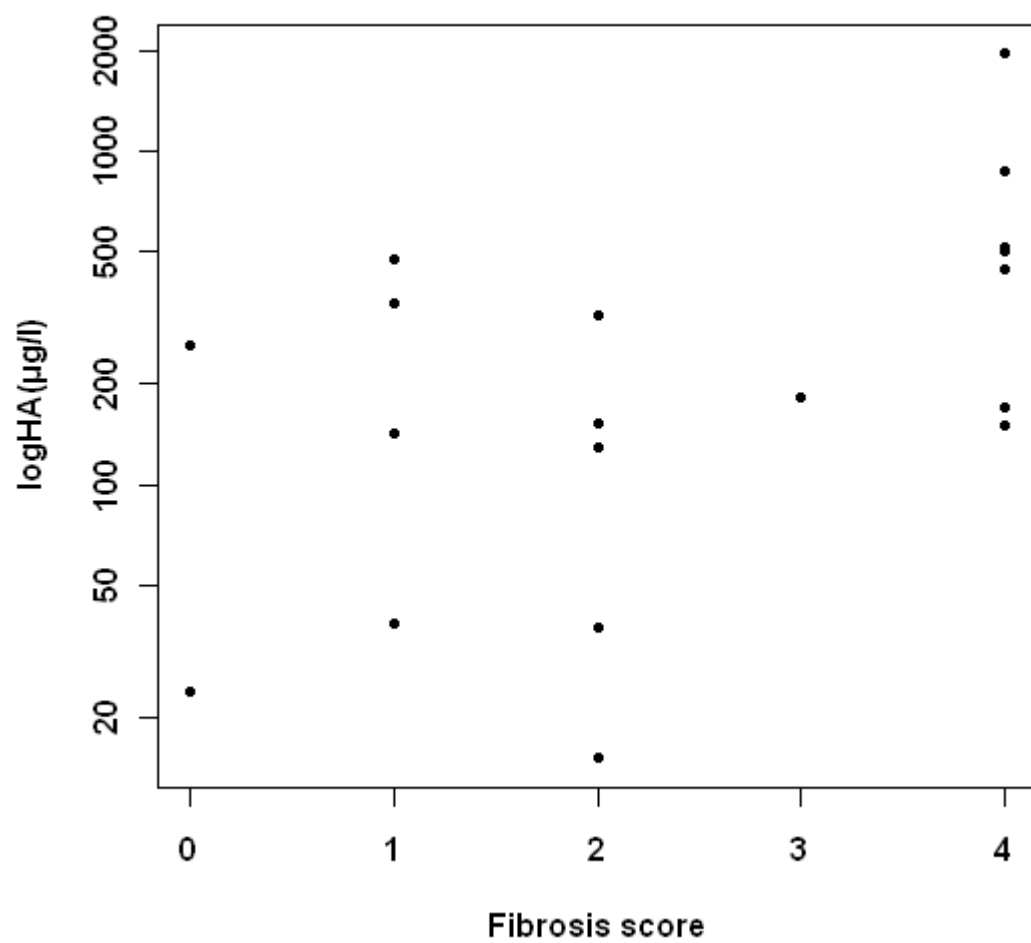


Figure 12

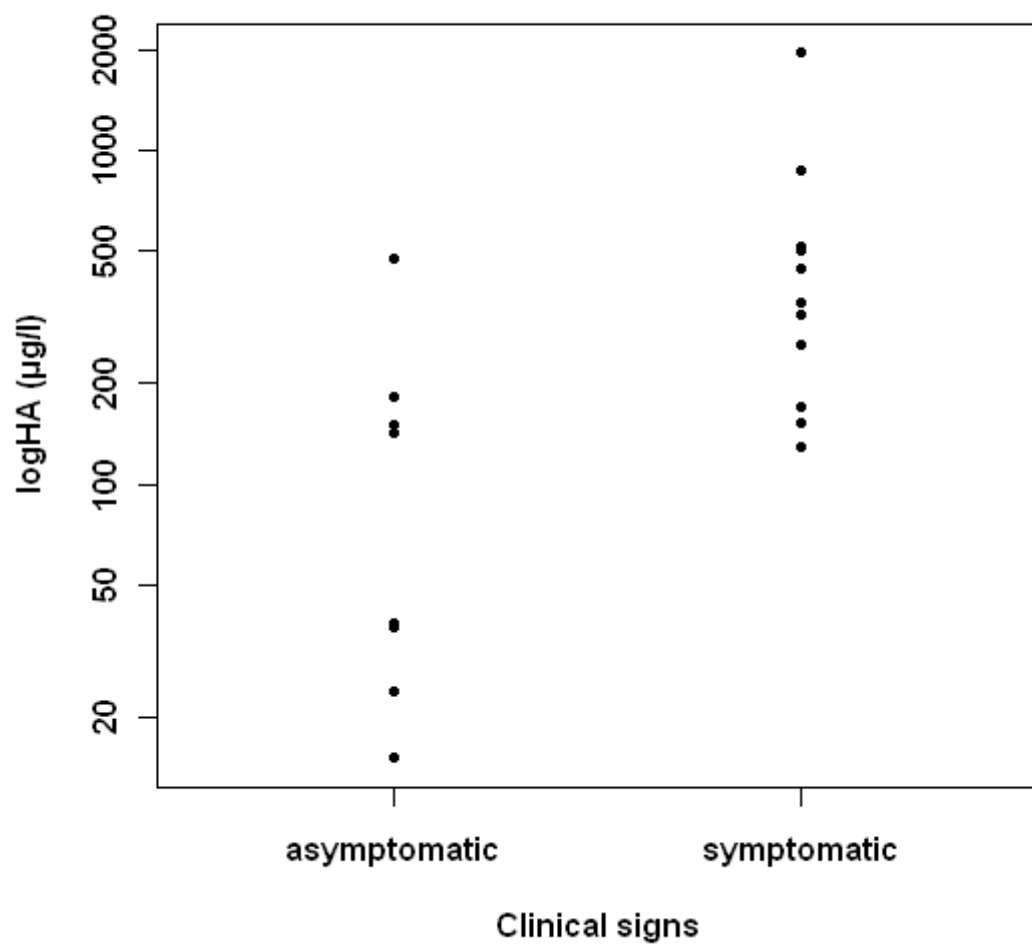


Figure 13

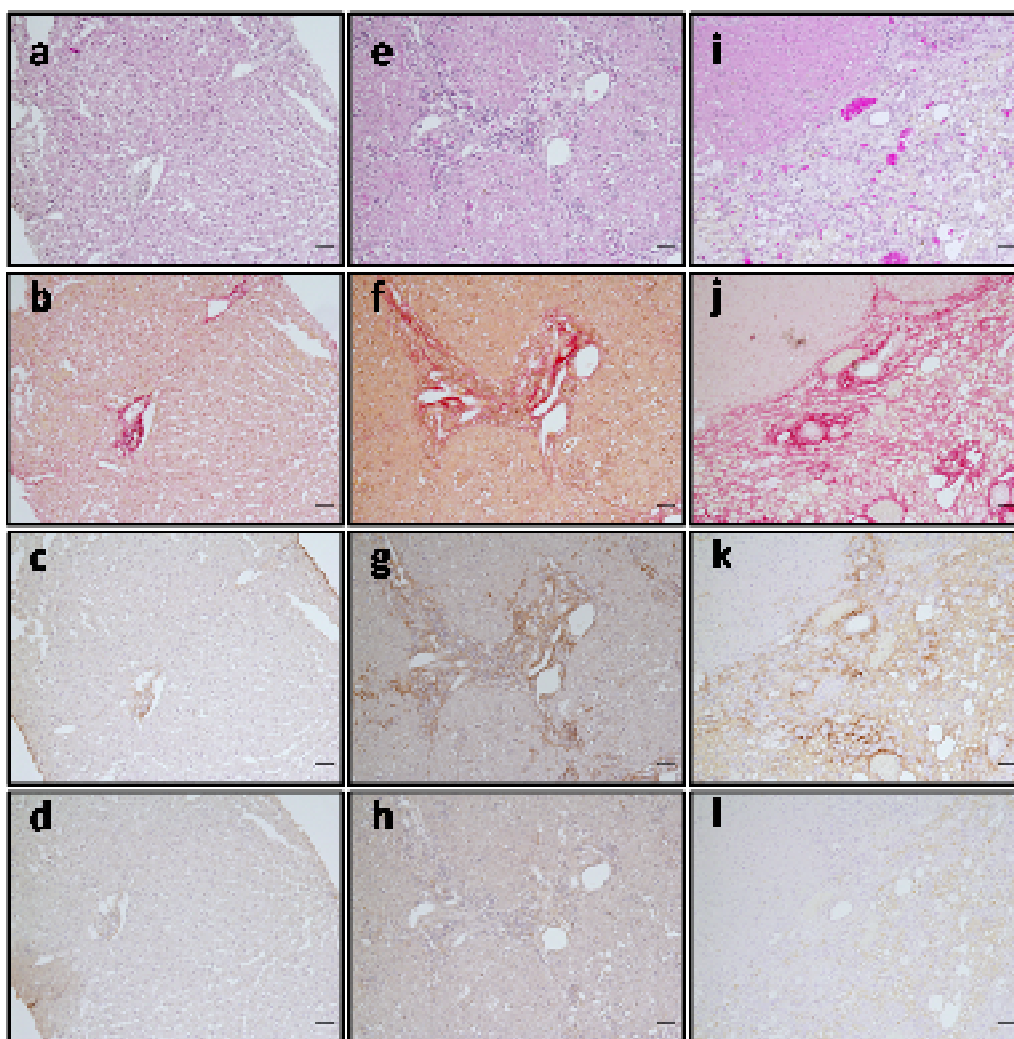


Figure 14

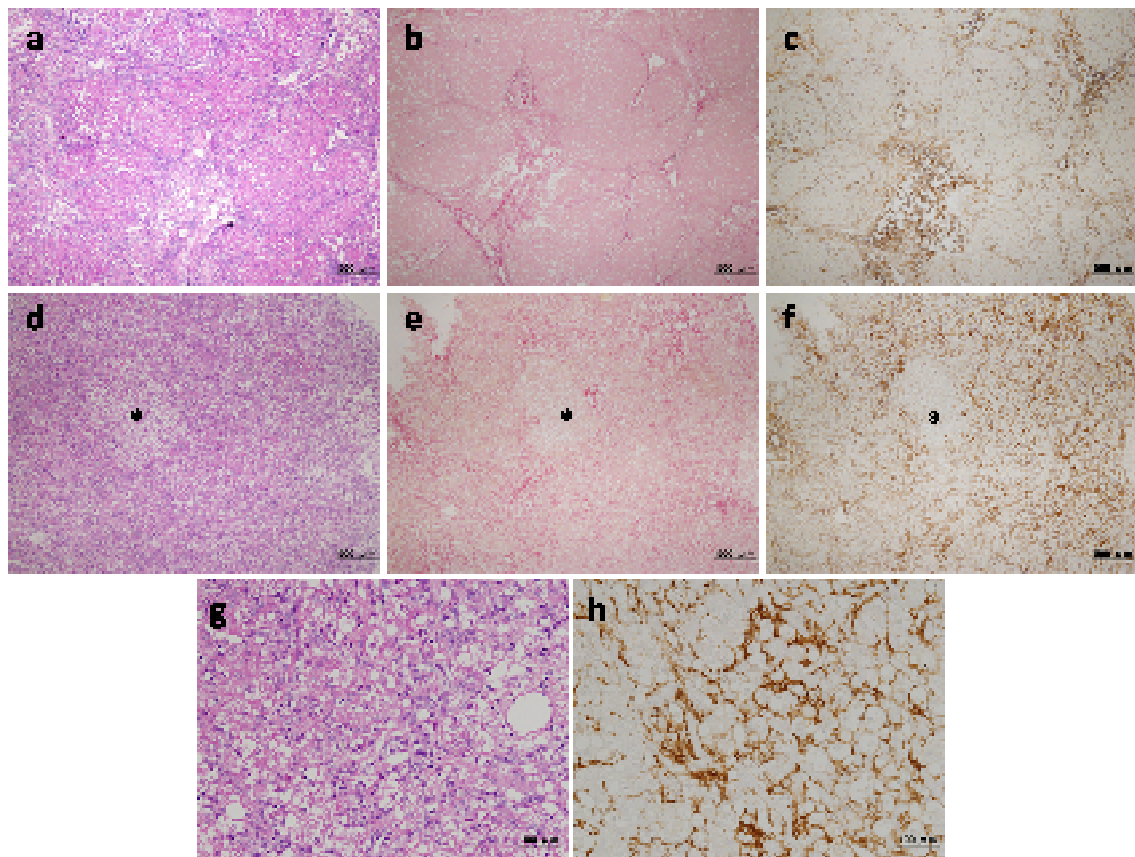


Figure 15

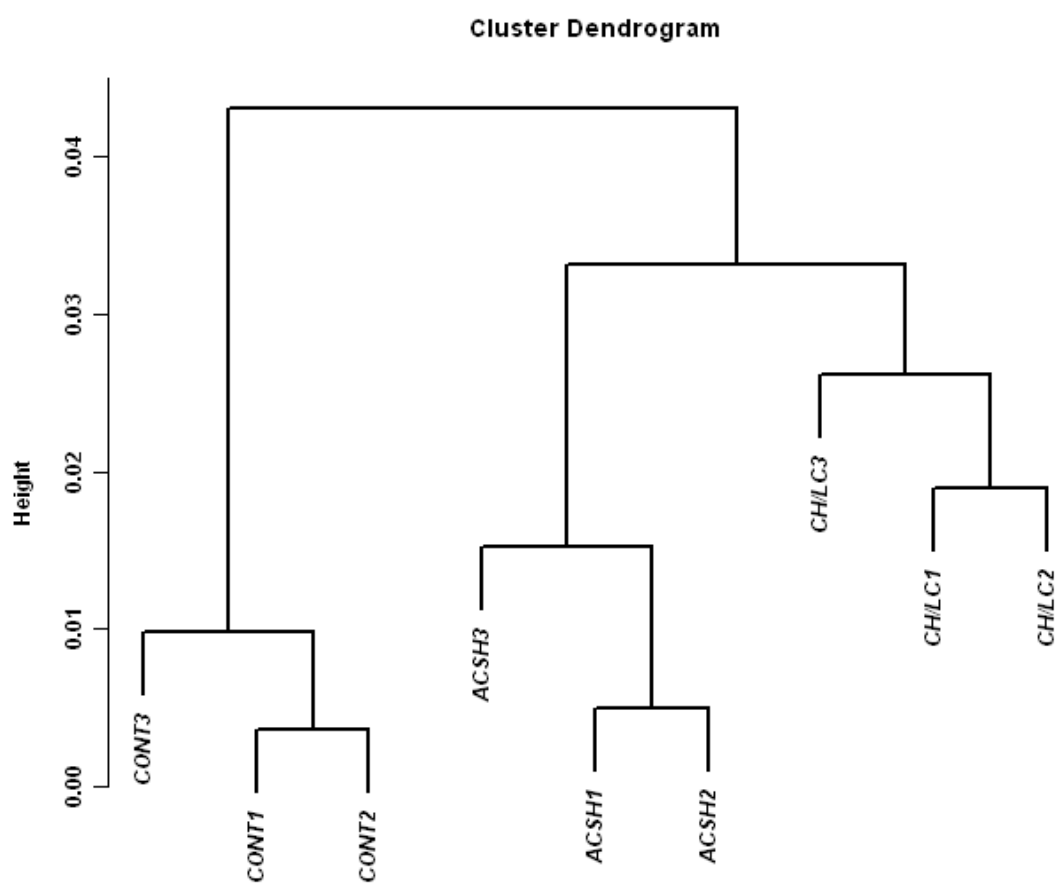


Figure 16

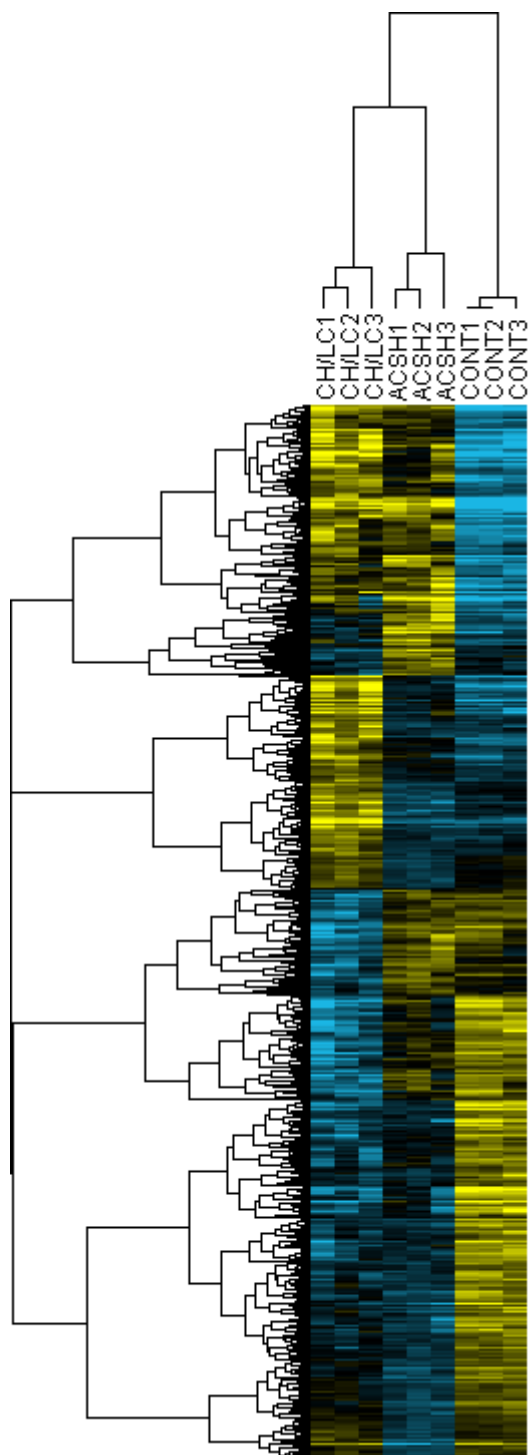


Figure 17

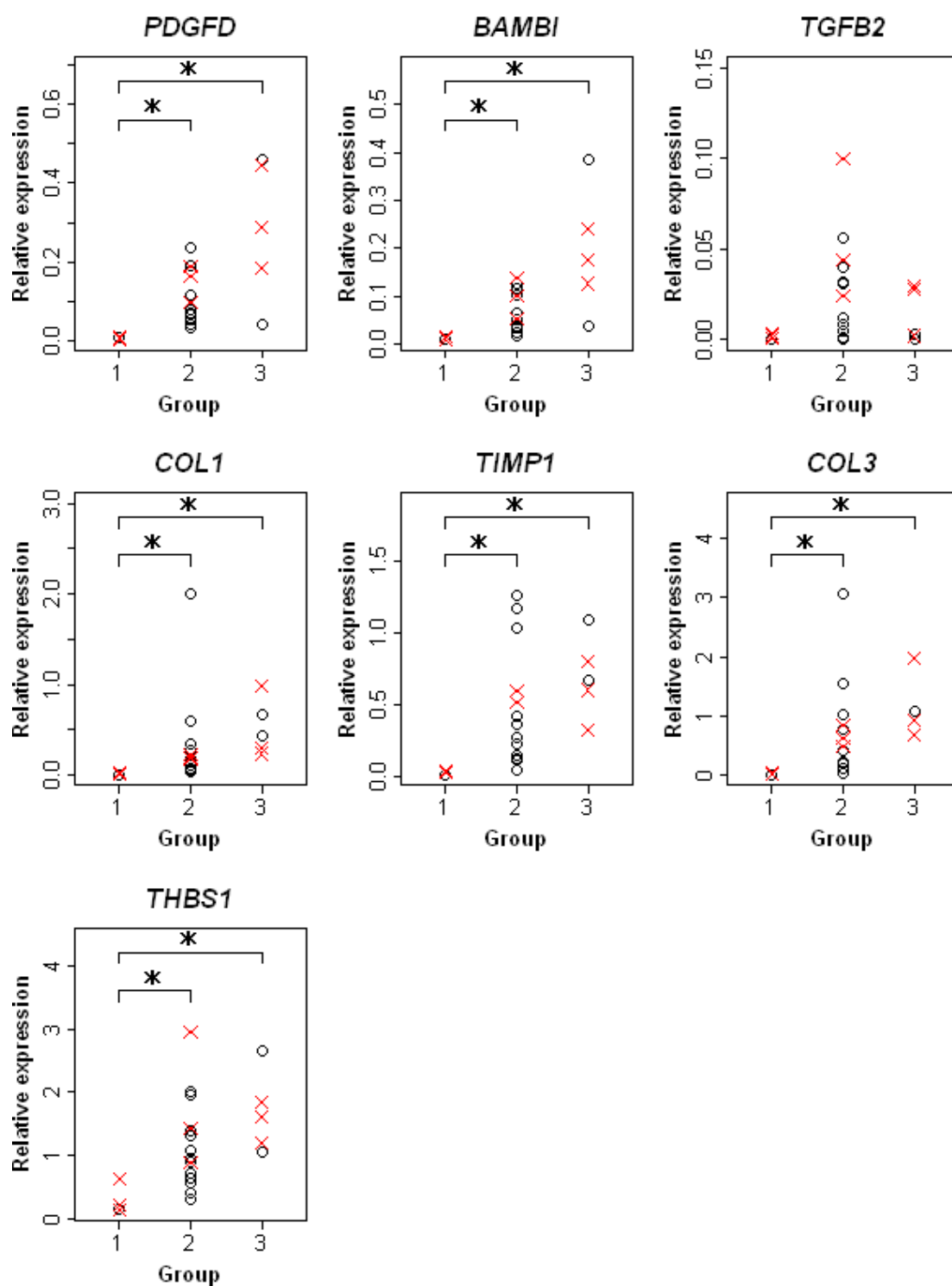


Figure 18

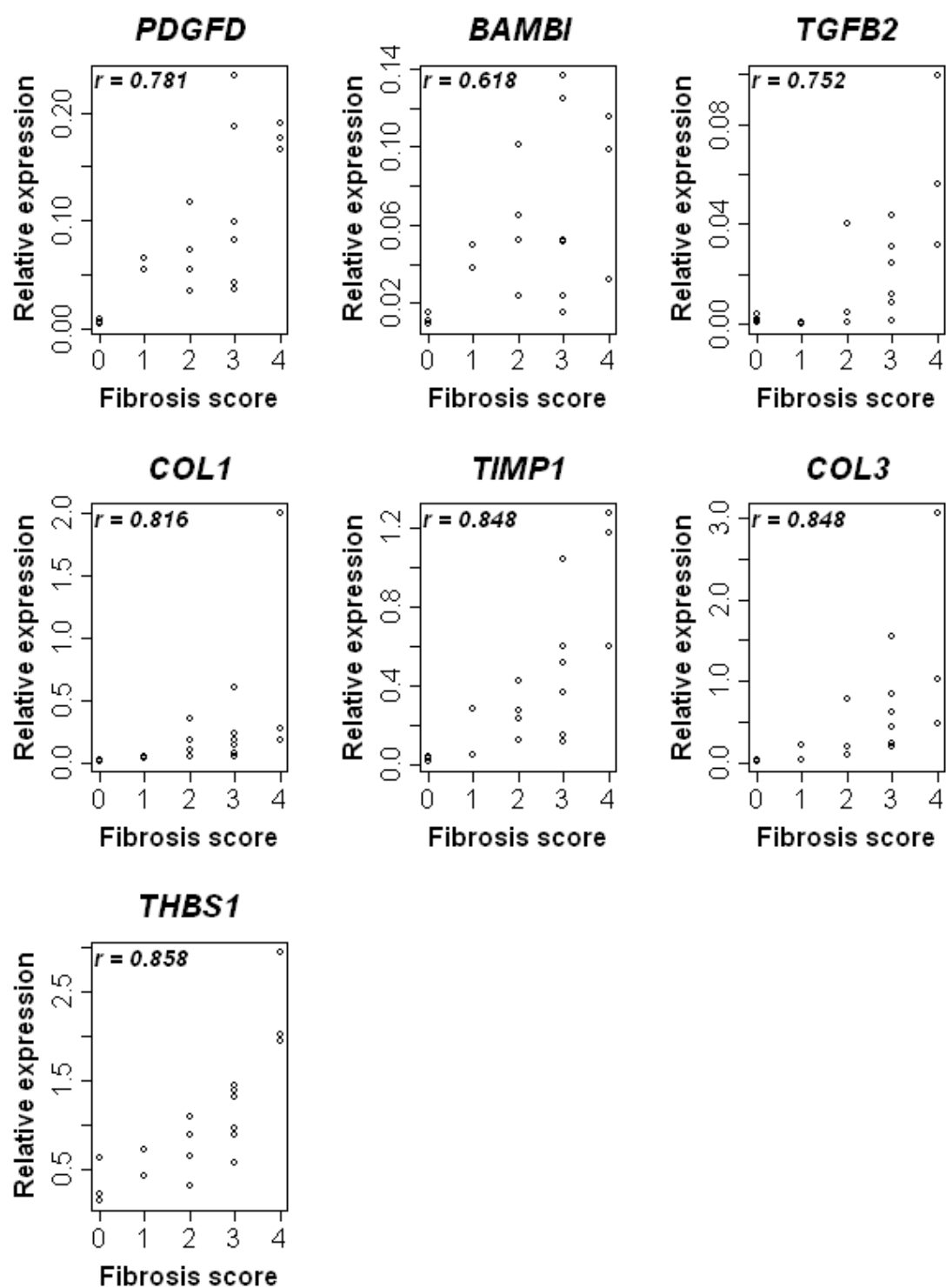


Figure 19

